

27  
3-2-77  
copy 1015  
IS-4033

MASTER

CROSSED-MOLECULAR BEAM APPARATUS  
TIME-OF-FLIGHT COMPUTER INTERFACE



T.P. Parr

AMES LABORATORY, USERDA  
IOWA STATE UNIVERSITY  
AMES, IOWA

Date Transmitted: January 1977

PREPARED FOR THE U. S. ENERGY RESEARCH AND DEVELOPMENT ADMINISTRATION  
UNDER CONTRACT W-7405-eng-82

DISTRIBUTION OF THIS DOCUMENT IS UNLIMITED

## **DISCLAIMER**

**This report was prepared as an account of work sponsored by an agency of the United States Government. Neither the United States Government nor any agency Thereof, nor any of their employees, makes any warranty, express or implied, or assumes any legal liability or responsibility for the accuracy, completeness, or usefulness of any information, apparatus, product, or process disclosed, or represents that its use would not infringe privately owned rights. Reference herein to any specific commercial product, process, or service by trade name, trademark, manufacturer, or otherwise does not necessarily constitute or imply its endorsement, recommendation, or favoring by the United States Government or any agency thereof. The views and opinions of authors expressed herein do not necessarily state or reflect those of the United States Government or any agency thereof.**

## **DISCLAIMER**

**Portions of this document may be illegible in electronic image products. Images are produced from the best available original document.**

CROSSED-MOLECULAR BEAM APPARATUS  
TIME-OF-FLIGHT COMPUTER INTERFACE

T. P. Parr

Ames Laboratory, ERDA  
Iowa State University  
Ames, Iowa 50010

Date Transmitted: January 1977

PREPARED FOR THE U. S. ENERGY RESEARCH AND DEVELOPMENT  
ADMINISTRATION UNDER CONTRACT NO. W-7405-eng-82

—NOTICE—  
This report was prepared at an account of work sponsored by the United States Government. Neither the United States nor the United States Energy Research and Development Administration, nor any of their employees, nor any of their contractors, subcontractors, or their employees, makes any warranty, express or implied, or assumes any legal liability or responsibility for the accuracy, completeness or usefulness of any information, apparatus, product or process disclosed, or represents that its use would not infringe privately owned rights.

DISTRIBUTION OF THIS DOCUMENT IS UNLIMITED

**NOTICE**

This report was prepared as an account of work sponsored by the United States Government. Neither the United States nor the United States Energy Research and Development Administration, nor any of their employees, nor any of their contractors, subcontractors, or their employees, makes any warranty, express or implied, or assumes any legal liability or responsibility for the accuracy, completeness, or usefulness of any information, apparatus, product or process disclosed, or represents that its use would not infringe privately owned rights.

Available from: National Technical Information Service  
U. S. Department of Commerce  
P.O. Box 1553  
Springfield, VA 22161

Price: Microfiche      \$3.00

Paper Copy      \$5.00

## TABLE OF CONTENTS

	iv
	Page
ABSTRACT	iv, v
INTRODUCTION	vii
APPARATUS AND EXPERIMENTAL	1
APPENDIX I.	39
APPENDIX II.	41
APPENDIX III.	42
REFERENCES	56
PROGRAM LISTING	57

## ABSTRACT

A variety of the gas phase reactions of barium and tin atoms have been studied using a crossed molecular beams machine with a universal quadrupole mass filter based detection system incorporating a time-of-flight (TOF) spectrometer for velocity analysis. Center-of-mass (CM) reactive product recoil angle and relative recoil energy distributions have been measured for the following reactions: 1)  $\text{Ba} + \text{N}_2\text{O} \rightarrow \text{BaO} + \text{N}_2$  2)  $\text{Ba} + \text{CO}_2 \rightarrow \text{BaO} + \text{CO}$  3)  $\text{Ba} + \text{O}_2 \rightarrow \text{BaO} + \text{O}$  4)  $\text{Sn} + \text{Cl}_2 \rightarrow \text{SnCl} + \text{Cl}$  5)  $\text{Sn} + \text{CH}_3\text{I} \rightarrow \text{SnI} + \text{CH}_3$  6)  $\text{Sn} + \text{n-C}_3\text{H}_7\text{I} \rightarrow \text{SnI} + \text{C}_3\text{H}_7\text{I}$  and 7)  $\text{Sn} + \text{CCl}_4 \rightarrow \text{SnCl} + \text{CCl}_3$ . At relative collision energies below  $15\text{kJmole}^{-1}$ , the BaO product of reaction 1) is seen to be sharply backwards scattered with only 10 to 20% of the total available energy in product recoil energy. These results are consistent with near 100% efficiency for production of electronically excited BaO. Evidence of a significant effect of  $\text{N}_2\text{O}$  vibrational energy on the total reactive cross section is presented. Reaction 2), at collision energies as high as  $31\text{kJmole}^{-1}$ , and reaction 3), at a collision energy of  $13\text{kJmole}^{-1}$ , both seem to proceed via a long-lived complex, and their product recoil energy distributions are reasonably well fit by the transition state theory of Herschbach et. al. No evidence of a  $\text{CO}_2$  internal energy effect on the total reactive cross section for reaction 2) was found. The SnCl product

of reaction 4) was predominately forward scattered with low product recoil energy; the SnI product of reactions 5) and 6) were sharply backwards scattered with relatively high recoil energies; the SnCl product of reaction 7) was sideways scattered. Thus the reactions of tin atoms studied here are very similar to the corresponding alkali and alkaline earth metal atom reactions. A minicomputer interface for collection and display of TOF spectrums and product angular distributions was built using a Digital Equipment Corp. PDP8/e computer and is described here in detail.

## INTRODUCTION

This report describes a time-of-flight spectrometer system for a crossed molecular beams machine utilizing a PDP8/e computer for on-line collection and display of data. Detailed descriptions, circuit diagrams, and program listings are presented. This report constitutes a chapter from the authors thesis, and is printed as an IS report so that the system, remaining at ISU, may be understood. The abstract lists those chemical reactions that have been studied with this system while at ISU. Further detail on these studies may be found in the author's thesis, from the University of California, Berkeley.

Distribution List

T. Parr -----	24
ERDA-TIC-----	27
ERDA-COO-----	1
Ames Laboratory Library -----	<u>8</u>
Total	60

## APPARATUS AND EXPERIMENTAL

### A. General Description

The crossed molecular beam machine used in this investigation is a modification of one designed by Y. T. Lee<sup>1</sup>, and the details of its design criteria and construction have already been discussed<sup>5</sup> by R. Behrens<sup>2</sup>, who was responsible for the building of this apparatus. For the benefit of the reader, a brief description of the machine will be given here along with a more detailed description of the portions of the experimental set-up for which the author was responsible.

The two molecular beams are produced in two source chambers as shown in figure 1 with the following exception; the source in source chamber 2 is not a nozzle gas source as shown but a high temperature oven designed by A. Freedman, described in his thesis<sup>3</sup>, and shown in figure 2.

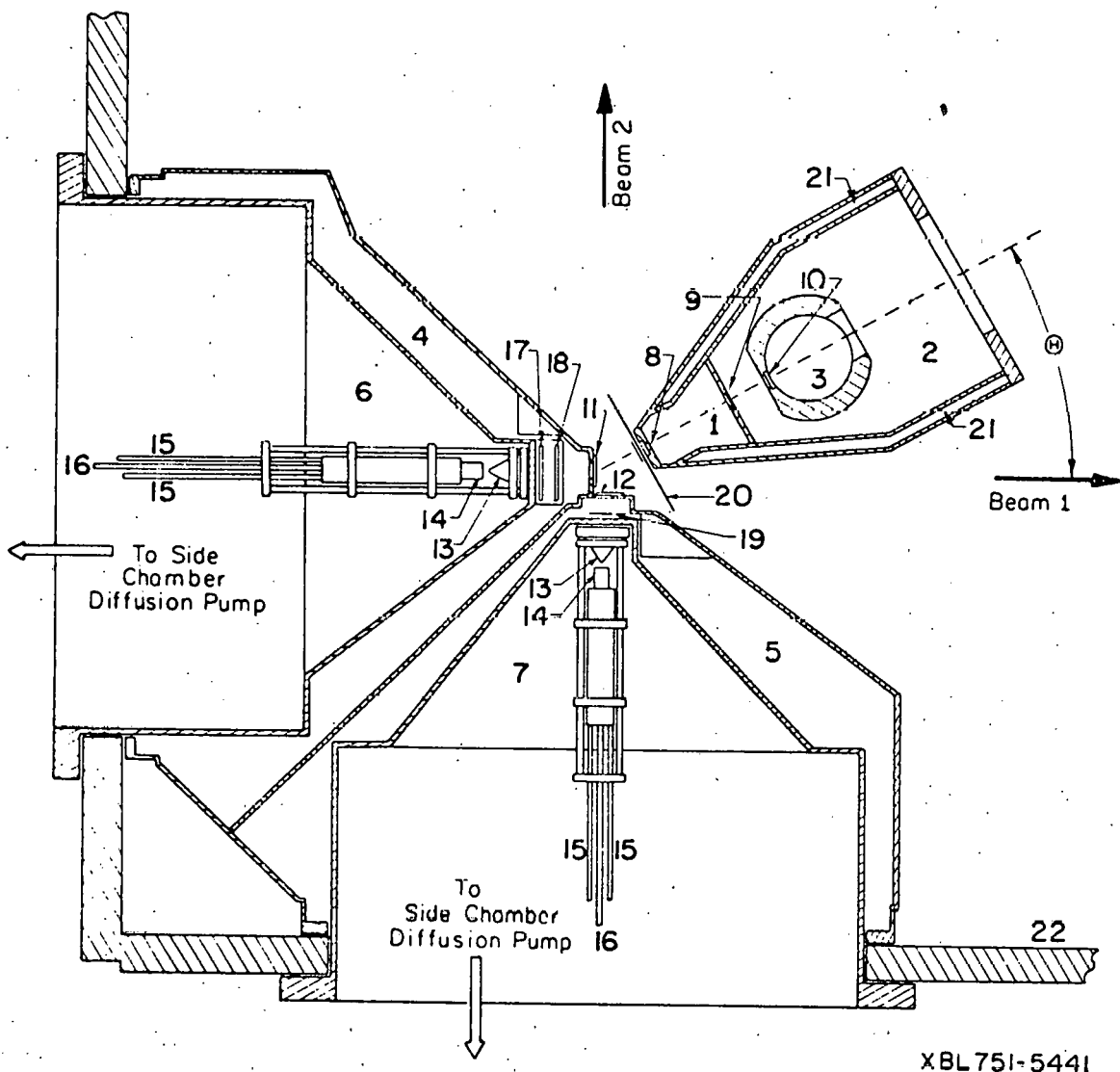
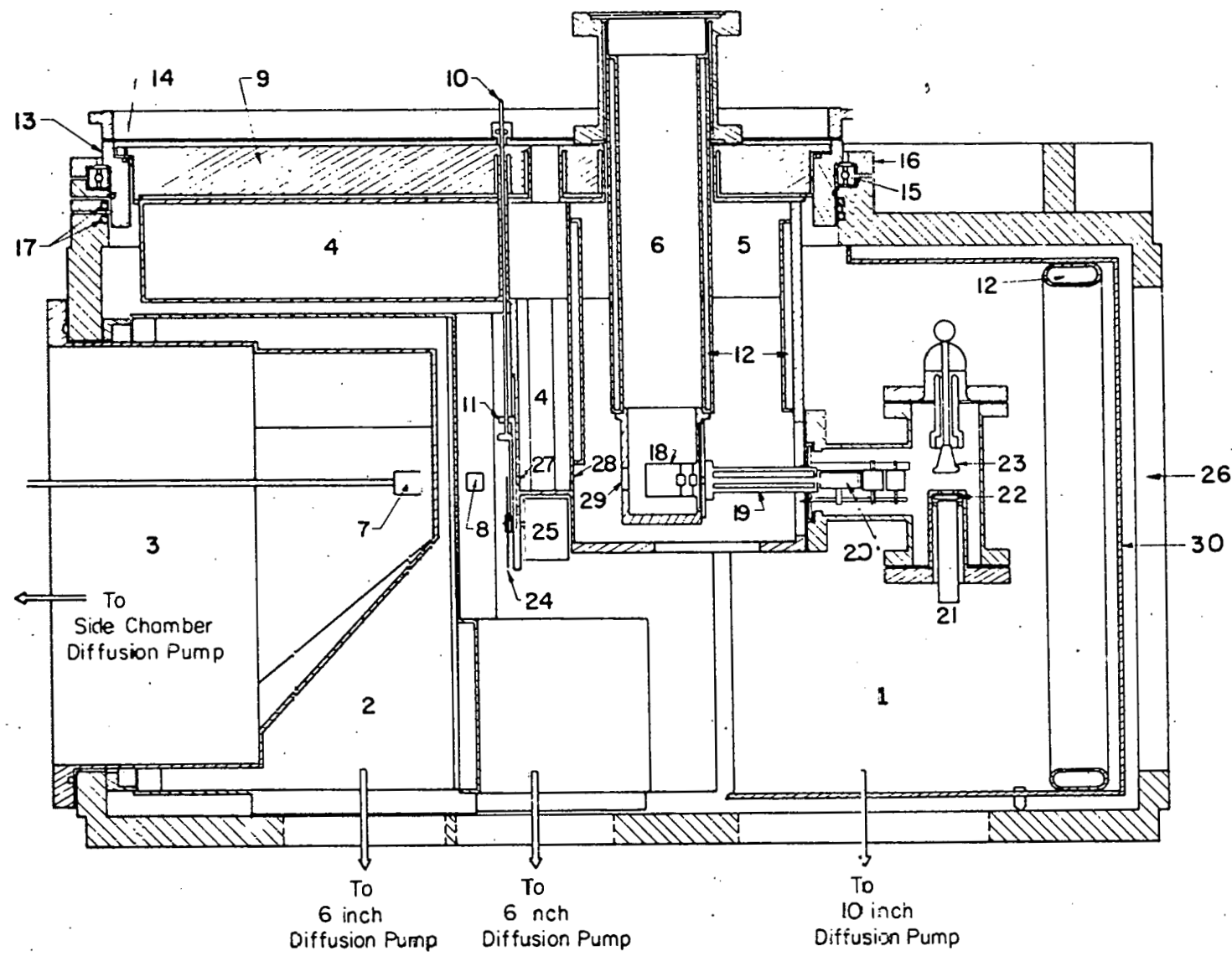


Fig. 1 A. Top Cross Sectional View of the Apparatus

Figure IA. Top Cross Sectional View of the Apparatus

1. Detection Chamber No. 1.
2. Detection Chamber No. 2.
3. Ionization Chamber.
4. Collimation Chamber 1.
5. Collimation Chamber 2.
6. Source Chamber 1.
7. Source Chamber 2.
8. Detector Chamber 1 entrance slit.
9. Detector Chamber 2 entrance slit.
10. Ionization Chamber entrance slit.
11. Beam 1 Collimating slit.
12. Beam 2 Collimating slit.
13. Skimmers
14. Nozzles
15. Heating or cooling fluid tubes.
16. Gas inlet.
17. Beam Flag 1.
18. Beam chopper
19. Beam Flag 2.
20. Time-of-flight wheel.
21. Liquid nitrogen cooling.
22. Main Chamber.



XBL 751-5449

Fig. 1 B. Cross Sectional View of the Apparatus

Figure IB. Cross Sectional View of the Apparatus

1. Main chamber.
2. Collimation chamber No. 2
3. Source chamber No. 2.
4. Detector chamber No. 1.
5. Detector chamber No. 2
6. Ionization chamber.
7. Nozzle source No. 2.
8. Beam source No. 1.
9. Rotating detector lid.
10. Gate valve drive rod.
11. Detector gate valve.
12. Liquid nitrogen cooling reservoirs.
13. Rotating ring.
14. Rotating lid O-ring seal.
15. Kaydon KG350XPO 35 inch bearing.
16. Bearing retainer ring.
17. Tec-Ring seals No. A-01926.
18. Ionizer
19. EAI Quad 250 quadrupole mass filter.
20. Quadrupole exit lenses.
21. EMI 9524S photomultiplier tube.
22. Pilot B plastic scintillator.
23. High voltage cathode.
24. Time of flight chopping wheel.
25. IMC time of flight motor.

Figure IB (cont'd).

26. Access port.
27. Detector chamber 1 entrance slit.
28. Detector chamber 2 entrance slit.
29. Ionization chamber entrance slit.
30. Cold shield.

## HIGH TEMPERATURE OVEN

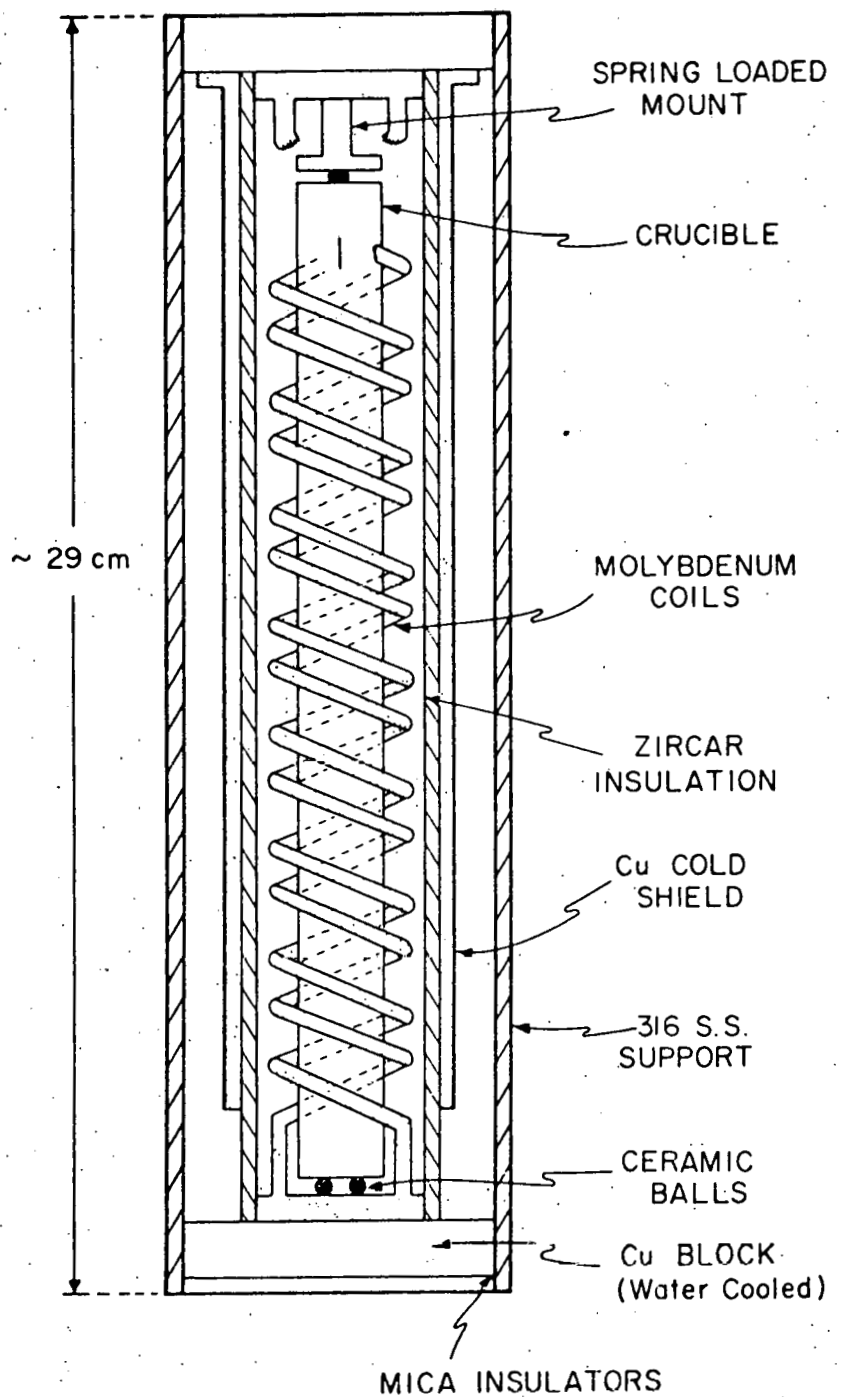


Fig. 2

Briefly it consists of, for the barium experiments, a molydenum crucible, 1.9 cm in dia and 25 cm long, that holds the charge, with a 0.025 cm slit 0.5 cm long cut in the face as shown. The lid of the crucible is welded shut to prevent any barium effusion or creepage from the top of the crucible, a problem with press fit lids. The crucible is heated radiatively by molydenum resistance heating coils wound around it operating at typical power levels of between 1 and 2 kW depending on the desired temperature. Wound around, but not touching, the heating coils is a layer of Zircor<sup>4</sup> insulation, which is contained by a copper cold shield connected to water cooling. In front of the oven is a solenoid operated beam flag. For the tin experiments the molydenum crucible had to be replaced because the molten tin literally dissolved and alloyed with the molydenum. At first a quartz liner for the molydenum was tried, but the tin reacted with the quartz, turning it white and crystalline and producing a strong tin oxide component to the beam. Finally a crucible almost identical in design to the molydenum one but made from graphite was tried with great success. This crucible, shown in figure 3, employed a press fit lid which showed no signs of leaking, and could be easily reopened after a run without damaging either the lid or the crucible. Furthermore the graphite showed no signs of being attacked or penetrated by the tin (the old crucible showed signs of the tin diffusing through the moly so that the whole surface acted as a source rather than just the slit). The slit in the graphite crucible was cut by mechanical means, rather than the electron beam discharge cutter used on the molydenum; for this reason it is wider - 0.5 cm versus 0.25 cm.

5/8



6-32 TAPPED HOLES FOR  
LID REMOVAL

INTERIOR CAMPHOR ANGLE IS  $4^\circ$

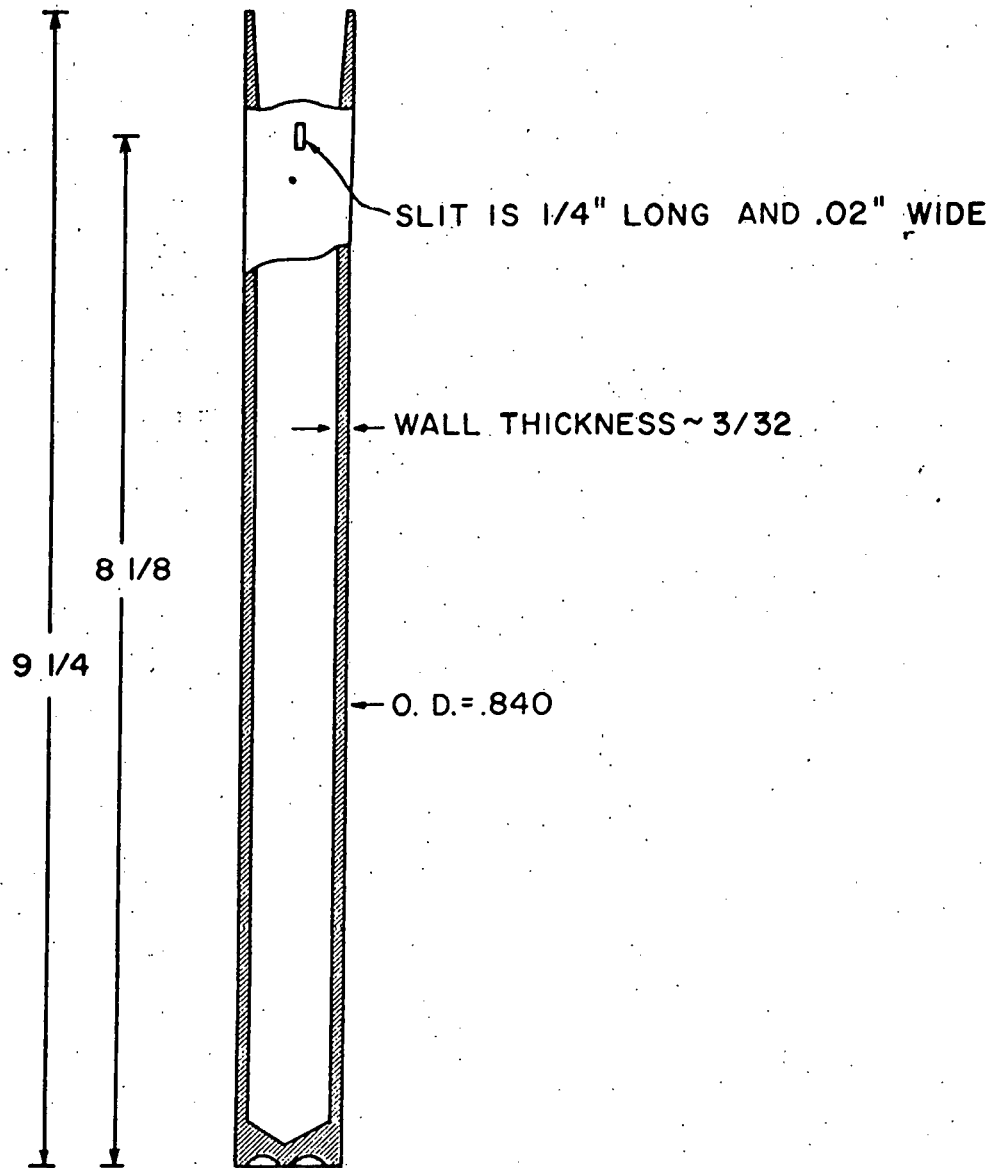


Fig. 3. Graphite Crucible

Since this oven certainly doesn't need the benefits of a differently pumped collimation chamber, the inside source chamber part 7 of figure 1 is removed and the oven source is mounted in the collimation chamber 2 which becomes the source chamber now pumped by the 10" side chamber oil diffusion pump through a 20" dia stainless steel e.l shaped chamber. The mounting is such that the slit in the crucible is 16.2 cm from the collimating slits (12 of figure 1) and 8.5 cm from the beam collision region. The collimating slits are two strips of Ta ribbon 0.2 cm apart and the geometry is such that the beam has an angular FWHM of 1.83 degrees and a special FWHM at the collision region of 0.27 cm for the barium experiments and the same for the tin experiments. (For the tin experiments the umbra is smaller and the penumbra larger, giving the same FWHM.

The other change involves the removal of the inside source chamber 1 (part 6 figure 1) and the remounting of the supersonic nozzle skimmer assembly (for a description see ref 2) on the collimation chamber on the back face of the now removed collimating slits (part 11). This was done in order to increase the intensity of the nozzle beam at the collision zone since it now placed the skimmer opening only 2.76 cm and the nozzle (which can be moved back and forth with respect to the skimmer) at a typical 4.11 cm from the collision region, compared to previous skimmer and nozzle distances of 10.5 and 11.9 cm respectively. Since the intensity of the beam falls off as the inverse of its distance to the collision zone squared one would expect an 8 fold increase in signal and attenuations in the new configuration. The best way to compare beam intensity in the two configurations is to look at how much the nozzle beam attenuates the oven beam. In the old configuration we could never really measure any substantial attenuation, less than 1%, unless the source

pressure was turned up so high as to swamp the diffusion pump or the nozzle moved very close (less than 2 nm) to the skimmer (both procedures causing adverse broadening of the beam speed distribution). Furthermore in the old configuration the nozzle beam never made any measurable rise in the main chamber pressure suggesting that not much beam was getting into the main chamber. In the new configuration we typically run with between 1 and 4% attenuations with reasonable source pressures (between 200 and 300 torr) and turning on the beam would cause the main chamber pressure to rise from a typical background pressure of  $4 \times 10^{-7}$  torr to between 1 and  $2 \times 10^{-6}$  torr. This is just the pressure rise expected according to a simple calculation based on the measured attenuation and main chamber pumping speed estimates. Some of this improvement was due to the use of larger diameter nozzle and skimmer orifices, and was made at the expense of beam angular resolution; the new configuration was calculated to have a FWHM angular spread of 7° compared to the old configurations 0.8°. The 7° wide beam is suitable for reactive scattering where fine angular resolution is not needed, but is unsuitable for some elastic scattering studies where poor angular resolution would wash out the details of the angular distribution (see ref. 5). Another disadvantage of this configuration is that there is now no room for the beam flag and beam chopper as shown in figure 1 (parts 17 and 18), and to chop the beam a solenoid, (actually a relay), with a metal flag attached, is mounted on the main chamber face of the collimation chamber so that when not energized it blocks the beam's path to the collision zone and when energized it allows the beam to pass. The disadvantage is that when blocked the deflected beam still passes into the main chamber in the vicinity of the collision zone and might react with the barium or tin on surfaces surrounding the collision zone, either the collimation chambers or the detector. The

products of these surface reactions might be picked up by the detector and cause negative signals i.e. signals larger when the beam is off than on, that would invalidate the single collision reactive signal desired. No evidence of this problem was observed except with the bromine time of flight experiments discussed later. Also discussed later, in Appendix I, are the details of the nozzle beam geometry.

With the inside source chamber 1 removed, the nozzle beam is pumped by both the 10" CVC oil diffusion pump via the el chamber and the 6" NRC oil diffusion pump at the bottom of the collimation chamber. (The 10" pump is backed by a KDM-65 mechanical and a KMB 230 booster pump; the 10" diffusion pump on chamber 2 by a KDM-80, and all other diffusion pumps by KC-15 mechanical pumps manufactured by Kinney vacuum.) Typical source chamber 1 pressure while operating the nozzle is  $2 \times 10^{-4}$  torr.

The two beams pass into and collide in the main chamber made, as are almost all components of this machine that are in vacuum, of stainless steel, and pumped by a cyrogenically baffled 10" CVC oil diffusion pump and indirectly by a 6" NRC pump. Typical main chamber background pressure is  $5 \times 10^{-7}$  torr. The size of the main chamber, 132 cm x 130 cm x 84 cm, was dictated by the size of the rotating lid, housing the detector. Inside the main chamber, encompassing the region that the detector rotates in, is a cyrogenically cooled copper cold shield, affording large pumping speed for condensable gases ( $\text{LN}_2$  temperatures). (The area between the cold shield and main chamber is a semi-sealed region pumped by the aforementioned 6" NRC oil diffusion pump and the nozzle beam strikes a beam deflector and is pumped out through this region unless the detector is in the way.)

The detector is housed in a triply differentially pumped cryogenically cooled vacuum chamber made of stainless steel and mounted on an 89 cm dia lid in a horizontal plane defined by the two beams, from  $-8^\circ$  to  $105^\circ$  where  $0^\circ$  is defined as the nozzle beam (source 1). The rotating seal consists of two Teflon Tec-Ring gaskets (Tec Seal Corp.). The detector entrance slit (figure 1 part 8) is 0.380 cm square and 4.44 cm from the collision zone, (for measuring the beams another slit is available which is only 0.008 cm in diameter to decrease the intensity of incoming gas and prevent overload of the detector). This chamber is pumped by an Ultek 150 l/sec ion pump, backed by a titanium sublimator, and the next chamber (2 on figure 1) surrounds the ionizing chamber and is pumped by a Vecco 225 l/sec ion pump, backed by a titanium electron beam sublimator. The third chamber (3 of figure 1) houses the ionizing portion of the mass spectrographic detection system, is liquid nitrogen cooled, and pumped by a Vecco 100 l/sec noble gas pump and by a liquid He pump not used in these experiments... typical background pressures in this chamber are  $2 \times 10^{-9}$  torr. The detection system consists of an axial electron bombardment ionizer housed in chamber 3 and constructed so that particles from the collision region which enter and are not ionized pass out through the back, are pumped away in chamber 2, and do not contribute to the background gas near the ionizer. Particles that are ionized are drawn out and focussed by an electrostatic lens system to enter a quadrupole mass filter and ions of the selected mass are passed out the back of the quadrupole and accelerated by a pair of lenses to strike an aluminum plated cathode held at minus 30 kV with respect to the energy of the ions. The resulting shower of ejected electrons are accelerated and strike an aluminum coated plastic scintillator causing

a shower of photons which are coupled to a photomultiplier tube (EMI 95245) producing a current burst at the output for each ion produced in the ionizer. The advantage of this system over using an electron multiplier to measure the ions is twofold: first the PM is sealed and therefore not subject to rather rapid degradation (by the corrosive gases used in some experiments) as open electron multipliers are. Second, each ion that strikes the Al cathode produces many electrons (estimated 2 to 6) which, when they strike the plastic scintillator, (Pilot B) produce about 12 photons; therefore each ion produces a burst of about 50 photons, and the problem of discriminating ion counts from stray light photon background counts becomes very easy. A disadvantage was that the high voltage needed for the cathode would cause electrical interference, by some form of non-sustaining discharge phenomena, that would cause the computer interface to malfunction. This was completely solved by electrostatically shielding all conductors of the high voltage inside the vacuum chamber. The current bursts from the PM tube are counted electronically by a system described later. The ionizer used for the barium experiments, similar in design to that of Brink<sup>6</sup> and designed and described by Behrens<sup>2</sup>, was normally operated at an electron energy of 60 V, electron current of between 10 and 15 mA and had an estimated ionizing region length of about 4 cm. The ionizer for the tin experiments, an Extranuclear Labs Model 041-1, was normally operated at 100 V electron energy and 5mA emission, and had an estimated ionizing length of 0.5 cm. For looking at the beams the emission was dropped to between  $10\mu$  A and  $100\mu$  A for both ionizers. Although not carefully measured (a difficult procedure), the typical ionizing efficiency of this type of ionizer lies between 0.01 and 0.1 so the probability of ionizing a particle is directly proportional to the length

of time it spends in the ionizer and therefore inversely proportional to the particles velocity causing the detector to measure a number density as opposed to a flux. (Particles per sq. cm per sec. times inverse velocity bias equals particles per cubic cm.) The quadrupole mass filter used for the barium experiment was an Electronics Assoc. Inc. Model Quad 250 along with its associated driving electronics. The quadrupole used in the tin experiments was an Extranuclear Labs Model 4-270-9 with Models 11, 13 and 15 Hi-Q heads and Models 020-2, and 011-15 driving electronics. The motivation for the change was hoped increased sensitivity of the companion ionizer, better resolution of the mass filter, and more accurate and stable mass selection ( the EAI mass filter's calibration was non-linear and changed frequently enough to make hunting for a mass peak an annoying procedure).

#### B. AC Syncronous Detection

Along with the reactive signal coming from the collision region there is also present at the output a background signal due to background gas in the detector or in the main chamber. One way to subtract out this background, or baseline, is to measure it before the beams are on and subtract that quantity from all later measurements, but this assumes that the baseline is constant with time. A better method, the one used here is to constantly measure this baseline by periodically interrupting the nozzle beam and accumulating the baseline count in one set of counters and the signal plus baseline count, when the beam is not interrupted, in a different set of counters. The difference between the two will then be that portion of the signal that depends on the collision of the beams without any added baseline. (An even better method, judged too complicated in this application, would be to chop both beams and measure the signal

at the beat of the two chopping frequencies; this would subtract all components of the signal not dependent on having both the beams on and colliding.) The duty cycle (time of beam on/total time) was chosen to be 50% for reasons of simplicity. (50% is not always the optimum duty cycle: if the baseline is very small or zero there is of course no point in measuring it so the optimum duty cycle would be 100%. It can be shown, appendix II, that the optimum duty cycle is equal to  $(S+B)/(S+2B)$  where S and B are the signal and baseline rates respectively.) Although one would like to have a high chopping frequency so as to average out fast drifts in the baseline, the frequency is limited by the spread in flight times of the beam particles from the chopping mechanism to the collision region and to the detector. There may be a sharply defined burst of particles at the chopping mechanism but since some travel faster than others, both in the beam and after they have reacted at the collision region, they may get to the detector before the slow particles from the previous pulse arrive; the phase information has been lost and synchronous detection won't work. For an idea of the time scale involved we make the more stringent requirement that we will discard all counts obtained for that amount of time past each beam on or off transition such that all but the slowest few percent of the particles in the beam have time to get to the detector. With a typical distance of 7 cm and typical slow velocity of  $5 \times 10^3$  cm/sec we get 1.4 msec, so a chopping frequency of 180 Hz would be wasting half the counting time on waiting for this "dead time".

In the original configuration of this machine, the beam was chopped using a motor driven wheel with slots in it that interrupted the beam in the collimation chamber as shown in figure 1 (part 18). An advantage of this system was that when the beam was chopped off all of it was pumped away in the collimation chamber and none got into the main

chamber to cause the previously discussed negative signals, from surface reactions. (A lesser advantage is that only half the total beam winds up in the main chamber as background gas.) A disadvantage was that the motor was inside the source chamber and the relatively high concentration of corrosive gases (when running such gasses in the nozzle) caused frequent failure of the motor bearings. Another disadvantage was, as previously mentioned, the nozzle had to be further away from the collision zone causing less beam intensity, so it was moved up to the collimation chamber face and the new beam chopper, mounted in the main chamber, was used. This beam chopper (the metal flag mounted on a relay) is much slower than the rotating wheel because, mechanically, the relay won't move much faster than a few cycles per second. A chopping period of 200 msec on and 200 msec off was chosen with 20 msec thrown out at each transition to allow the flag to move into position and the transients (the flag oscillates slightly) to die down. (The chopping frequency could be made much slower, all the way to DC, but problems would develop with the computer interface to be discussed later.)

### C. Time of Flight Spectrometry

The system described so far measures the reactive signal as a function of scattered angle. It is also useful to measure it as a function of the velocity of its constituent particles. For inelastic scattering studies this velocity distribution, giving a translational energy distribution, would be helpful in elucidating the energy transfer mechanism being studied. The translational energy distribution of reactive scattering would also be helpful in elucidating the total reactive product energy partitioning, an important part of microscopic kinetics. Finally the velocity distribution of the beams and scattered signal are needed to form the Newton diagram

and transform the differential cross section from the lab to the more meaningful center of mass frame of reference (see chap. 3). Therefore it would be advantageous to have some device that specifies or selects velocity in conjunction with the rotatable lid that selects angle.

Conventional velocity selectors operate on a time of flight principle and consist of arrays of slotted disks, arranged in series on a common shaft, and spun by a variable RPM motor. The disks are precisely aligned so that only those particles within a certain small velocity range will traverse through the slots without hitting any of the tines and being deflected out of the path to the detector. The selected velocity range is varied by changing the motor RPM and the resolution is given by the construction of the slotted disks. These selectors are however, too big to incorporate in most rotatable detector molecular beam machines, and furthermore since it takes considerable time to complete a velocity sweep, changing beam conditions could distort the measured velocity distributions. A much simpler way to obtain velocity information is by means of a single slotted disk, spun so that it allows short bursts of molecules to enter the detector. Each of the molecules in the burst travels the distance,  $d$ , between the slotted disk and the ionizer portion of the detector, where they are ionized and quickly detected. It is obvious that the faster ones get there sooner than the slow ones. The signal at the detector therefore consists of a burst of counts, where each count is delayed from the initial pulse by a time  $t = d/v$ ,  $v$  being the velocity of the particular molecule being counted and  $d$  being the distance from the slotted disk and the detector. This "time of flight spectrum", i.e. the intensity of counts as a function of flight time, can be inverted to obtain a velocity distribution, since the flight distance,  $d$ ,

is known. See eq 1 where  $I(t)$  and  $I(v)$  are intensities as a function of time and velocity respectively.

$$\text{eq 1)} \quad \left| \int I(v) dv \right| = \left| \int I(t) dt \right| \Rightarrow I(v) = I(t) \left| \frac{dt}{dv} \right| \Rightarrow I(v = \frac{d}{t}) = \frac{I(t)t^2}{d}$$

Notice that the resolution for this method of velocity measurement is poorest for highest velocities i. e.  $dv = \frac{v^2}{d} dt$

The slotted disk, shown in figure 1 as part 20 and called the "time-of-flight" wheel (TOF wheel) is mounted below the detector so that the slots pass directly in front of the detector opening. (The wheel is spun by an AC synchronous hysteresis motor.) It is 14 cm in diameter and the diameter to the center of the detector opening is 13.2 cm. The perfect TOF wheel would let through an infinitely narrow (both time and therefore special) burst of particles for maximum possible time, and therefore velocity, resolution. It would also have an unusable zero transmission, defined as percentage open time. If the fractional time resolution is defined as the open time for each slot (being equal to the uncertainty in starting time for each burst of particles) divided by the period between slots (being the total time scale of the TOF spectrum), it is obvious that the fractional time resolution is equal to the transmission. It can also be seen that the absolute resolution is given by the fraction transmission times the wheel period divided by the number of slots. It is also given by wheel period times slot width divided by total wheel circumference. If the fractional resolution is made better by decreasing the slot size then the transmission will suffer; if the transmission is then made larger by increasing the number of slots then another problem, wrap-around, will occur. Wrap-around occurs when the burst of particles

from one slot comes before all the particles from the previous burst have gone the flight distance and been counted by the detector, thus falsely showing up as very high velocity particles rather than their true slow velocity. The actual design of the wheel was chosen as follows. First the gate function, the transmission of the wheel as a function of time, actually depends on the size of the hole in the detector as well as the slot size of the wheel. In fact the convolution of the square slot passing in front of the square detector hole produces a trapezoidal gate function. In the case of equal sizes, the design chosen was both equal to 0.38 cm, the gate function is a triangle. If the wheel slot size is made much smaller than this the transmission (for a given wrap-around condition) will suffer while the fractional resolution will now, due to the convolution with the hole in the detector, not get much better. (Example: if the slot is halved in size the transmission is halved but the gate function total width is only decreased by 25%). If the slot is made much larger the resolution will suffer, so equal sizes were chosen as a compromise. The number of slots was governed by the maximum RPM of the motor and the requirements of wrap-around problems. The maximum motor RPM was about 12500 because above that vibration of the motor was transmitted through the lid to the ion pumps causing pressure bursts and instabilities and increasing the background count rate. Thus at maximum RPM, and therefore maximum absolute resolution, the wheel period was 4.8 msec. In order to give a TOF spectrum length of 1.2 msec, very adequate protection against wrap-around even for the heaviest and therefore slowest molecules such as tin iodide, a wheel with four slots was chosen, each slot being the previously mentioned 0.38 cm wide. Another good choice would have been six slots giving a minimum TOF spectrum length of 0.8 msec, but this would have necessitated slowing the wheel down and decreasing the absolute resolution when wraparound became a problem. (The wheel must have an even number of slots for reason of balance and for reasons pertaining

to the interface to the computer.) From the above design it can be seen that the wheel has a transmission of 3.7% and a minimum gate function of  $0.44 \mu\text{secs FWHM}$ . (For a velocity of  $5 \times 10^4 \text{ cm/sec}$  this is a resolution of  $(5 \times 10^4)^2 (4.4 \times 10^{-6}) / 19.3 = 5.7 \times 10^2 \text{ cm/sec}$ , which is using the previously given equation  $dv = V^2 dt/d$ .

Not yet mentioned in this discussion is the flight distance  $d$ , which is the distance from the TOF wheel to the center of the ionizing region of the ionizer. There is an uncertainty in the flight distance given by  $\pm 1/2$  the length of the ionizing region. For the barium experiments the average  $d$  and uncertainty are 19.3 and  $\pm 2 \text{ cm}$  and for the tin experiments 18.85 and  $\pm 0.250 \text{ cm}$  owing to the different ionizers used<sup>3</sup>. The gate function (uncertainty in flight time due to uncertainty in starting time) and the length of the ionizing region (uncertainty in flight distance) cause the measured TOF spectrum to be broader than the true spectrum. In fact the measured spectrum is a complicated two dimensional convolution of the true spectrum with the gate function and the ionizer length. A program to deconvolute the measured to obtain the true spectrum has been written by A. Freedman and is discussed in his thesis<sup>3</sup>.

A TOF parameter of lesser importance is the delay time from ionizing a particle and detecting it as a pulse from the photomultiplier, basically the time it takes an ion to drift through the quadrupole at some given ion energy  $V$  (measured as the difference in potential between the ionizer grid and the quadrupole or ground). Since the actual fields involved are not known, the delay time can be given approximately by the equation  $t(m) = k \sqrt{M/V} (Mv^2 \alpha V, t \propto 1/v, \text{ so } t \propto \sqrt{M/V})$  where  $M$  is the ion mass (gm molecular weight) and  $V$  is the ion energy (volts). If the TOF spectrum of species

of two different mass, yet assumed same velocity distributions, are taken, then the constant  $k$  can be determined:

$$t(M_2) - t(M_1) = k \left\{ \sqrt{M_2/V} - \sqrt{M_1/V} \right\} = \Delta t \quad \text{so}$$

$k = \Delta t \left\{ \sqrt{M_2/V} - \sqrt{M_1/V} \right\}^{-1}$  where  $\Delta t$  is the difference in time between the peaks of the two TOF distributions. For example the TOF spectrums of  $SF^+$  and  $SF_5^+$ , both from fragmentation of  $SF_6$  in the ionizer, were measured and the peaks differed by 15  $\mu$ secs. Therefore  $k = 15 \left\{ \sqrt{127/23} - \sqrt{51/23} \right\}$  or  $k = 2 \times 10^{-5} \text{ sec } V^{1/2} \text{ gm}^{-1/2}$  valid for the tin experiments (done on the ENI ionizer and quadrupole.) For the barium experiments  $k = 1 \times 10^{-5}$ . For a typical ion energy of 60V and mass of 153 (BaO) this would give an ion flight time of 16  $\mu$ secs a small correction.

#### D. Cross Correlation TOF Spectrometry

Another TOF technique, not used here due to lack of time for conversion, is cross correlation TOF spectrometry, with the added advantage that the transmission is always 50% regardless of the resolution<sup>7,8</sup>. (50% transmission, compared to 3.7%, would require only 7% of the counting time.) This method would also involve a slotted disk spun in front of the detector opening, as before, except that the disk would be divided into 127 equally spaced regions and the presence of a slot or a time would be given by a pseudo-random maximal length binary sequence. These sequences of binary numbers are finite in length,  $N=2^n - 1$ , where  $n$  is an integer, and possess many of the properties of random white noise. The auto correlation function for each sequence, over the length of the sequence, approximates a delta function ie is equal to -1 for all time shifts other than zero for which it is equal to  $N$  (discrete sum rather than integral. The autocorrelation of true random noise is a delta function.) Although the output of the detector will now look like random noise, the time of flight spectrum can be extracted

by cross correlating the output signal with the pseudorandom gating function.

Suppose we have a constant incoming signal of  $K$  gated by a gate function

$A_n = 1/2 (G_n + 1)$  where the subscripts denote discrete steps in time equal to the time for one time or slot to pass the detector hole and also equal to the bin time of the measuring system (discussed below).

$G_n$  is the pseudorandom sequence taking on values of +1 or -1; therefore  $A_n$ , the gate function, takes on values of +1 or 0 (open or closed).

The signal measured by the detector will be the convolution of the gate function and the response function of the particles i.e. their TOF spectrum  $h_n$ .

$$S_n = K \sum_{m=1}^N 1/2(G_{n-m} + 1)h_m$$
 which is to say that the signal at some time  $n$

is equal to the gate function at time  $n$  times the response function for zero time (infinite velocity) plus the gate function for previous times multiplied by the response function for non-zero flight time. Now to extract the TOF spectrum,  $h_m$ , we cross correlate  $S_n$  with  $G_n$ :

$$R_{SG} = \sum_{n=1}^N S_{n+p} G_n = \frac{K}{2} \sum_{n=1}^N \left[ \sum_{m=1}^N (G_{n-m+p} + 1)h_m \right] G_n$$

$$= \frac{K}{2} \sum_{m=1}^N \left[ \sum_{n=1}^N (G_{n-m+p} + 1) G_n \right] h_m$$

but  $\sum G_{a-b} G_a = N$  if  $b=0$ ,  $= -1$  if  $b \neq 0$ , and  $\sum_{n=1}^N G_n = +1$

$$\text{so } R_{SG} = \frac{K}{2} \sum_{m=1}^N [(N+1) \delta_{m,p} - 1 + 1] h_m$$

$$R_{SG} = \frac{K}{2} (N+1) \sum_{m=1}^N \delta_{m,p} h_m = \frac{K}{2} (N+1) h_p$$

so TOF spectrum  $h_p = 2R_{SG}/K(N+1)$

The advantage in cross correlation TOF spectrometry are mainly the high transmission, 50%, and the variable resolution set by the motor RPM ( and theroretically arbitrarily small if it weren't for the finite size of the detector opening and finite ionizer length.) Another advantage can be seen by example when the cross correlation of the pseudorandom sequence and true random noise is taken and found to be proportional to the square root of- the sequence length,  $N$ . As seen above the cross correlation of a true signal is proportional to the sequence length + 1. Thus there is an improvement in signal to noise ratio, proportional to  $N$ . A disadvantage, also seen by example, is that statistical noise from a large peak in the TOF spectrum will be spread out by the cross correlation to all regions of the spectrum and possibly mask small ancillary peaks or at least make their signal to noise ratio worse. Thus this technique is most attractive when colorless TOF spectrum are anticipated, and least attractive when small peaks of interest are dominated by large peaks. Furthermore there is the problem of the design of the wheel. If the slot size is taken as 0.38 cm for reasons given before, then the wheel must have 127 "slots" since this number must be equal to  $(2^n - 1) \cdot m$  where  $n$  and  $m$  are integers. If a sequence length of 127 ( $n=7$ ) is chosen then only one sequence per circumference is allowed ( $m=1$ ), and this would mean that, at the maximum RPM of 12,500, the TOF spectrum would be taken out to an unrealistically long 4.8 msec. If a sequence length of 31 ( $n=5$ ) is chosen then four sequences can be included ( $m=4$ , No. slots=124) and the TOF period is 1.2 msec, but the added signal to noise improvement of longer sequences is lost. A solution to this would be to remount the motor to one side of the detector and use a larger diameter wheel. (The current 14 cm dia. wheel is mounted below the detector

and restricts angular movement between  $0^\circ$  and  $90^\circ$ . Mounting to the side would allow a 28 cm dia wheel and would restrict angular movement to one half the total range so that, if the wheel could be mounted on either side, the full range of angles could be reached by doing each experiment in two sections.) A good compromise design would be a 28 cm dia wheel with two sequences of length 63 giving a minimum TOF spectrum length of 12 msec and a minimum resolution twice as good as before (21  $\mu$ secs).

#### E. TOF Computer Interface

The time of flight (TOF) spectrum could be displayed on an oscilloscope; the horizontal sweep would be synchronized with the pulses from the slotted wheel, the horizontal axis would be the flight time  $t$ , and the vertical axis would be the intensity (signal from the detector). This will not work at all for scattered species because the signal is buried in too much noise. Some sort of signal averaging is needed, where many bursts of molecules are let into the detector and the time of flight spectrums from each burst are averaged together. This is best done by using a computer. The flight time is compartmentalized into "bins" where each bin has a width of  $\Delta t$  and the  $n^{\text{th}}$  bin corresponds to a flight time of  $n \cdot \Delta t$ . In reality these bins are locations in the computer memory. Counters count the signal occurring during the first bin's time  $t = 0$  to  $\Delta t$ , and add these counts to those already in the first bin; then they reset and count the signal occurring in the next  $\Delta t$  segment in time and add these to the contents of the next bin etc.; whenever the wheel opens up to let in another burst, the counters go back to the first bin and start over again. After a while the TOF spectrum builds up in the computer memory, where consecutive locations in memory hold data from consecutive flight times.

A block diagram of the time of flight system used by our group is shown in figure 4. (The interface is built with standard TTL circuitry and detailed schematics are shown in figures 5 to 13.) The computer used is Digital Equipment Corp.'s PDP 8/e. It is operated in the Direct Memory Access (DMA) mode using the one cycle data break for collection of data. Thus the collection of data is totally transparent to the program being run on the computer, which is usually a display routine that shows the developing TOF spectrum on an oscilloscope. A programmed interrupt system is used to transfer commands to the interface and to receive status signals from it.

As shown in the diagram, the experiment consists of two beams that are crossed to form a scattered signal which is passed through the rotating slotted disk to form short bursts of molecules. (A light bulb-photo diode assembly is mounted 180° away from the detector opening so as to generate an electrical signal that tells when the wheel is "open". A discriminator-line driver circuit shapes this pulse and sends it via coax to the computer as the "FAST WHEEL SIGNAL" (positive going pulses).) The molecules traverse the flight distance,  $d$ , and are ionized by the ionizer, selected as to mass by the quadrupole mass filter, and accelerated to strike the aluminum cathode by the exit lens. The Al cathode then emits a shower of electrons which, when they hit the scintillator, create a burst of photons, which is detected as a pulse by the photomultiplier tube. (Each of these pulses corresponds to a single ion from the ionizer.) The pulses are detected by the PM discriminator-line driver circuit and sent via coax to the computer as "DATA PULSES" (negative going pulses.). After the slotted wheel lets in a burst of molecules the fast wheel signal pulse resets the DMA address counters to zero. The contents of these counters specify, partially, what memory address in the computer will receive the data being transferred. (The rest of this address is given by the field control which sets bits 0 to 3 and is discussed later. A total of 512 locations are reserved for single precision data;

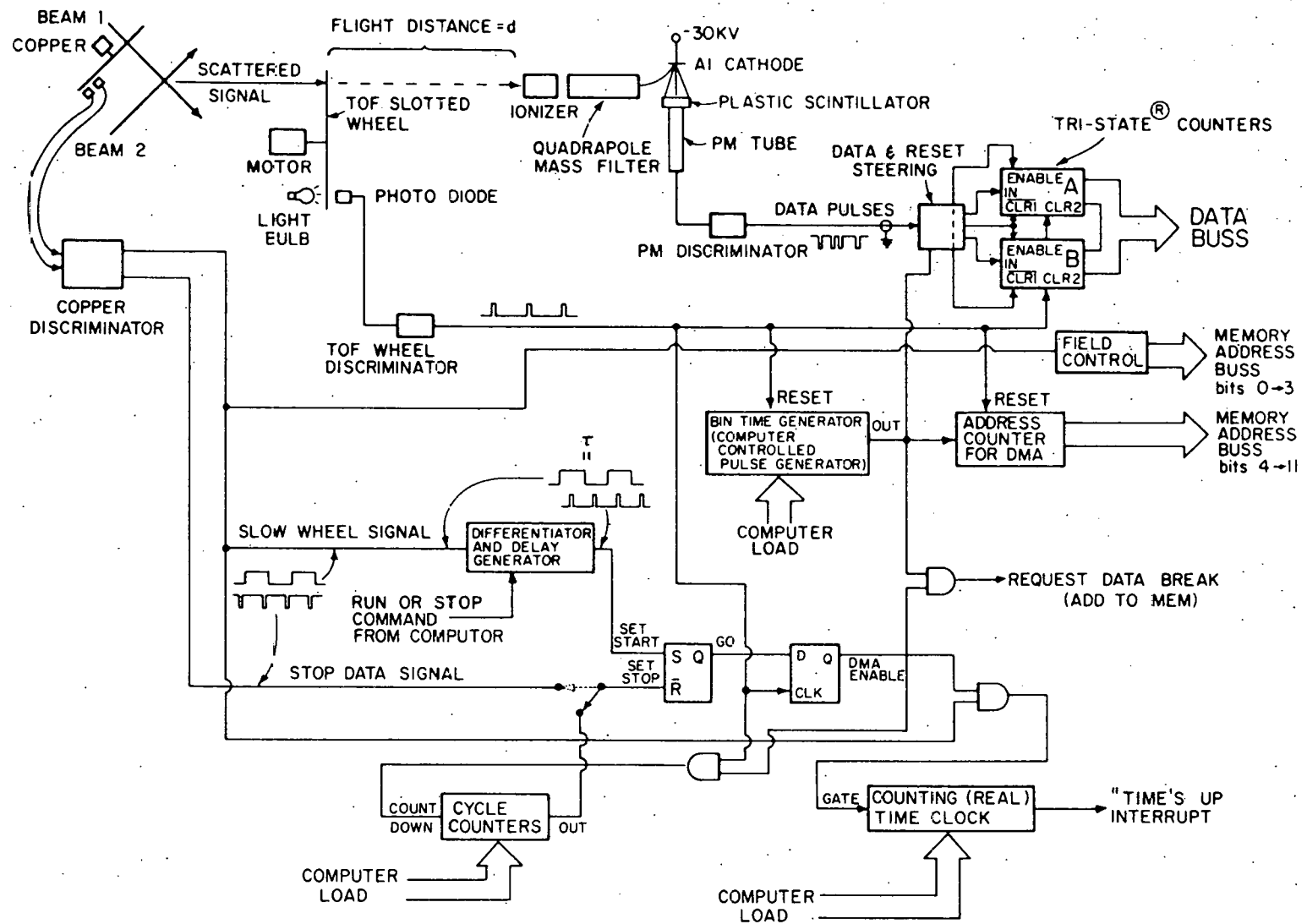


Fig. 4

256 for signal plus noise and 256 for noise.) The fast wheel signal pulse also reset plus noise and 256 for noise.) The fast wheel signal pulse also resets the data counters A and B and the bin time generator (BTGO which is a computer setable pulse generator. (The operator can load from the teletype keyboard whatever "bin time",  $\Delta t$ , discussed before, that he wants the BTG to generate.) After the fast wheel pulse the data gate sends the data pulses to data counter A. (These are Schottky TTL counters and can count up to 100 MHz although the PM tube in use can't get much above 5 MHz). After a time  $\Delta t$ , the BTG generates a pulse that initiates a number of things. First the data pulses from the PM disc are routed to the B counter (identical to A counter). Also the address counter is incremented by one (address now equal to  $2001_8$  if beam on,  $2401_8$  if beam off), and a data break is requested of the DMA circuit. When the DMA circuit grants this request the contents of the address counter (and field control) are gated onto the memory address lines and the contents held in data counter A, those counts that occurred in the first  $\Delta t$  of the flight time, are added to the contents of memory location specified by the address buss. When this transfer is over, the A counter is cleared. Thus those counts destined for "bin number one" are loaded into the computer while the B counter is accumulating the counts to be added to bin number two. When the next BTG pulse comes, the process repeats except that the contents of the B counter will be added to bin number two (location  $2002_8$  or  $2402_8$ ) while the A counter accumulates bin number three's counts. This continues until the next fast wheel pulse\*, when the address is again set to zero and the cycle repeats. (note that this process of counting has zero dead time since one counter is accumulating data while the other is sending data to the computer.)

\* If the address counters go through all 256 locations before the next fast wheel pulse, they stop the data taking until the next fast wheel pulse comes.

From the above description it can be seen that the TOF spectrum will reside in the computer memory with the contents of each location being the intensity and the address of each location being directly related to the flight time  $t$ .

The majority of remaining circuitry of the interface is concerned with controlling the above data collection process i. e. telling the computer when to start and stop taking data. This is done syncronously with the "slow wheel signal", named for the beam chopping wheel used in the old configuration of the machine. As mentioned before, in the new configuration, the nozzle beam, beam 1, is chopped by a flag type chopper and the electronics that drives this relay chopper also generates the slow wheel signal, a 50 ohm TTL level signal that is 2.5V when the beam is open and OV when its blocked. The sequence of events is as follows: the operator types an "R" for run and the computer sends a RUN command to the interface. The next positive going transition of the slow wheel signal (i.e. beam turns on) is then passed through the differentiator (which generates a short positive going pulse for every transition of the slow wheel signal, either positive or negative) and then is delayed by a time  $\tau$  (internally set in the computer by a 20 msec one-shot). The delay time  $\tau$  is required to allow time for the beam flag to move since the slow wheel signal is coincident with the relay driving signal but the relay can't move instantaneously. (This delay time also allows time for the chopped beam to reach the collision zone and the detector as previously mentioned, thus eliminating transients in the TOF spectrum.) The delayed pulse then sets the GO flip-flop so that the next TOF wheel pulse will set the DMA ENABLE true allowing the BTG to generate data break requests and, in effect, initiating TOF data taking. Also enabled are the TOF wheel pulse CYCLE COUNTERS which, having been preset by the operator (through the keyboard) to some number  $N$ , now start to count down to zero.

When they reach zero they reset themselves to the number N and generate a narrow pulse that clears the GO flip-flop allowing the (negative going transition of the ) current TOF wheel pulse to clear the DMA ENABLE flip-flop thereby halting the data breaking process and stopping the TOF spectrum. On the next transition of the slow wheel signal (which would now be the beam turning off) the process repeats itself identically except that the field control is now set such that data are being added to the beam off field. (When the slow wheel signal is low the data field control output is 0101 for address bits 0 to 3 i.e. locations  $2401_8$  to  $2777_8$ . When high, (beam on), the data field is 0100 or locations  $2001_8$  to  $2377_8$  for the beam on field. ) The process continues to repeat itself until either 1) the operator types "S" for stop 2) the counting time clock times out and generates a TIME'S UP interrupt or 3) the overflow circuit (discussed later) generates an interrupt. In all of these cases the computer issues a stop command to the interface and the control circuitry is set such that the next positive going transition of the slow wheel signal is not allowed to restart data breaking. Therefore the computer stops taking data after having executed the same number of beam on as beam off cycles.

The TOF wheel CYCLE COUNTERS must be preset by the operator who must calculate the value of N beforehand as follows: the beam chopper is driven so that the open (and closed) time is 200 msec, subtracting the delay time of 20 msec gives 180 msec into which N TOF wheel cycles must fit. If the TOF period (from one pulse to the next) is 1.2 msec then  $N = 180/1.2 = 150$  or 135 for a safety factor. Notice that the system is constrained to count exactly equal amounts of time with the beam on as off since the CYCLE COUNTERS always allow only N cycles of the TOF period per each half cycle of the beam chopper. (The counting time scale during each TOF cycle is governed by the crystal controlled BTG and so the beam

on and beam off counting times are precisely equal to each other to within almost the limits of reasonable measurement.) This feature was not operational for some of the early studies of this group.<sup>13</sup>

Note that the COUNTING TIME CLOCK, a real time crystal controlled clock that can be set, as an alarm clock, to generate an interrupt after any given amount of time between 0.2 and 200000 seconds, is only enabled during beam on data counting so that the count rate is the number of counts divided by the counting time.

The DMA system is used in the add to memory mode, i.e. the 12 bit content of the data counters is added to the 12 bit content of the selected memory location in the computer. If this sum should overflow into the 12th bit the hardware has been designed to generate an interrupt telling the computer that this has occurred and that further data taking would result in non-retrievable overflow errors. On receiving this interrupt the computer clears the run flip-flop so that data taking will stop on the next slow wheel on transition. After DMA'ing has stopped, the computer goes to a software double precision add routine that takes data existing in the single precision data fields and adds them to double precision data fields (locations 3002 to 3777 for signal plus noise and locations 4002 to 4777 for noise). After this is complete the computer restarts the data taking, with the single precision data fields now empty and ready to accept more counts.

The above description is for the mode in which the "fast wheel" is installed and the computer is taking time of flight data. It is also useful to remove the "fast wheel" and take angular distribution data. The advantage to this is higher total signal (increased by a factor of the inverse of the resolution of the particular "fast wheel"), and the ability to rotate the lid through a larger range of angles. The simple way to get the computer interface to operate in an angular distribution mode is simply to fool it into thinking it's taking TOF data. "Fake" fast wheel pulses are generated by a pulse generator set by the operator, (who then also recalculates and reloads N.) The computer is set up to run exactly as in the TOF mode. The only difference is that the display and printout routines are told to show

the total sum of all the addressed bins\*, which is the total signal (or signal plus noise or noise, depending on display mode) at the particular angle being looked at. (The bin number, bin time, velocity, and flux columns are ignored in this mode.)

As mentioned before, the computer system operates in both the direct memory access mode and the programmed interrupt mode. The DMA process is totally transparent to the program being run. The software written for this system consists of a background program that displays the developing TOF spectrum on an X-Y oscilloscope and a foreground program that services the interrupts generated by the interface and also transfers commands to the interface. A complete description of these programs can be found in the comment portion of the program listing. Briefly, the display routine can display either the single precision or the double precision data fields, either signal plus noise (beam on), noise (beam off), or the difference (signal). It can be told to display any number of points and can be told to average over (sum up) any number of consecutive points. This last feature is useful for very noisy signals where structure may become apparent if portions of the signal are averaged together, i. e. resolution is sacrificed for better signal to noise ratio. The display routine automatically scales both axis (to within a factor of 2). It can also inform the operator what full scale corresponds to in number of counts. The display routine is always running, even while data are being taken, so that the TOF spectrum can be seen to "grow".

The foreground program handles interrupts both from the interface and from the teletype keyboard. If the interface wishes to inform the computer

\*Actually the number of addressed bins minus 2 or 3 for a safety factor since the last bin is interrupted by the TOF pulse and is not always valid.

of something, it generates an interrupt and then the computer generates an Input Output Transfer that transfers a STATUS WORD into the accumulator. The computer then "interrogates" this status word where each bit has the following meanings. Bit zero active (equal to 1) means the bin time is too small i.e. the DMA system is attempting to data break faster than the computer can handle it. The computer will type "BIG TOO FAST" and the operator must reload the bin time generator (see Table I) with a larger time and hit "R" for run again. A reasonable minimum bin time is 5  $\mu$ secs (bintime must be in whole number  $\mu$ secs only) although the computer can go as fast as 3  $\mu$ secs if everything stays in sync.

Bit one active means that the prescribed counting time has elapsed. The computer stops the data taking and types out "TIME'S UP". The operator may then do one of several things. He may print out the data (see below). He may continue data taking for another prescribed counting time by pressing "R". If the present data do not look good the operator may erase them by pressing "K" and start over. Both the counting time clock and the bin time generator "remember" their values unless reloaded or unless the computer is turned off. The contents of the counting time clock can be read even while the experiment is running so the operator can see how much longer he has to wait. Also he may stop the experiment at any time (press "S") and read the CTC to see how long the experiment has been counting for. Loading the CTC entails an inaccuracy of about  $\pm 3\%$ , but reading the CTC gives the counting time exactly.

Bit two active signifies an overflow into the 12th bit while DMA adding to memory. The computer stops the data taking and then executes the previously described double precision add routine. After this is complete the computer restarts the data taking.

The computer can also send commands to the interface. They can be in the form of an IOT that transfers a command word to the interface. The details are shown in Table II.

The machine-operator interface consists of a teletype for input and output and the previously mentioned X-Y oscilloscope for output. The operator initiates computer operations by pressing a single key on the teletype keyboard. Some of these keys are "non printing" i. e. they transfer commands to the computer but the computer does not echo back anything so the Teletype does not print anything. Table I gives a list of all the keyboard commands. Any character other than those listed causes the computer to echo a carriage return and line-feed back to the Teletype. When loading numbers the format should be as described in "Introduction to Programming" Vol II floating point package DEC-08-YQ2B-B. (When loading the BTG only whole  $\mu$ secs are loaded. Thus 13.8 will be loaded as 13  $\mu$ secs.). Note that while the experiment is running, the computer should not be in the comment mode since the interrupt system is off in this mode and a computer won't be able to process a "TIME'S UP" or "OVERFLOW" interrupt. Note also that single precision data can be added to the double precision data at any time while the data taking is in process by pressing "L" (or "W"). If the experiment is "STOPPED", however, pressing either L or W will result in the computer adding single precision to the double precision data and printing out the double precision data. Note also the discrepancies listed under "N" (NUM. BINS) and "[ " (NS).

The "delay time" mentioned under "LOAD PARA" and "NS" is merely a constant that is subtracted off the accumulated bin time in the "WRITE DATA" program. For example, if the bin time is 10  $\mu$ secs and the delay time is  $-50$   $\mu$ secs then the first bin is at  $55$   $\mu$ secs, the second at 65  $\mu$ secs etc. The sense of this delay time is such that positive delay

Table I.

OPERATING INSTRUCTIONS FOR THE EXPERIMENT CONTROL PROGRAM

KEY	NAME	DESCRIPTION
A	NCYCLE	LOADS TIME TOF WHEEL PULSE COUNTER. HIT A, COMPUTER WILL TYPE "#CYCLES=", TYPE AND INTEGER HIT RETURN
B	BIN TIME	LOADS THE BIN TIME GENERATOR. HIT 'B', COMPUTER WILL TYPE "BT=", THEN OPERATOR CAN TYPE IN THE VALUE HE WANTS (IN MICRO-SECONDS). SEE 'INPUT FORMAT'.
C	CONTINUE	TELLS THE COMPUTER TO CONTINUE COUNTING AFTER HAVING BEEN STOPPED. DOES NOT RESET THE COUNTING TIME CLOCK. (IF CT=100 AND EXP. STOPPED AT 70, THEN HITTING 'C' WILL CAUSE COMPUTER TO CONTINUE COUNTING FOR 30 SEC.)
E	READ CTC	CAUSES COMPUTER TO PRINT OUT THE CURRENT CONTENTS OF THE COUNTING TIME CLOCK, I. E. HOW LONG THE COMPUTER HAS BEEN COUNTING FOR.
F	FULL SCALE	CAUSES THE COMPUTER TO PRINT WHAT FULL SCALE (10 VOLTS) ON THE DISPLAY CORRESPONDS TO IN TERMS OF COUNTS. WORKS FOR ANY MODE OF THE DISPLAY ROUTINE.
K	KILL	ERASES DATA FIELD. 'RUN' DOES NOT DO THIS.
L	LOAD	CURRENTLY IDENTICAL TO 'W'.
N	NUM. BINS	LOADS THE NUMBER OF 'BINS' THAT THE COMPUTER DISPLAYS OR PRINTS OUT. HIT 'N', COMPUTER WILL NOT TYPE ANYTHING, OPERATOR CAN THEN TYPE IN WHAT HE WANTS. CURRENT DISCREPENCY: N IS THE NUMBER OF POINTS THAT THE DISPLAY WILL SHOW BUT THE WRITE OUT ROUTINE WILL ONLY PRINT UP TO BIN NUMBER N. THESE ARE NOT EQUIVALENT UNLESS 'NS' IS EQUAL TO ONE.
Q	QUEARY	CAUSES THE COMPUTER TO PRINT OUT THE STATUS OF THE EXPERIMENT: RUNNING OR STOPPED.
U	SINGLE PRE.	CAUSES THE DISPLAY ROUTINE TO LOOK AT THE SINGLE PRECISION DATA FIELD:
V	DOUBLE PRE.	CAUSES THE DISPLAY ROUTINE TO LOOK AT THE DOUBLE PRECISION DATA FIELD.
X	SIG. + NOISE	CAUSES THE DISPLAY TO LOOK AT BEAM ON DATA FIELD.
Y	NOISE	CAUSES THE DISPLAY TO LOOK AT THE BEAM OFF DATA FIELD.
Z	SIGNAL	CAUSES THE DISPLAY TO SHOW THE ARITHMETICAL DIFFERENCE OF THE BEAM ON AND BEAM OFF DATA FIELDS.
R	RUN	RESETS THE COUNTING TIME CLOCK AND THEN STARTS COUNTING.
S	STOP	STOPS THE EXPERIMENT.
T	COUNT TIME	LOADS THE COUNTING TIME. HIT 'T', COMPUTER WILL TYPE "CT=", THEN OPERATOR CAN ENTER THE AMOUNT OF TIME HE WANTS THE EXPERIMENT TO COUNT FOR. THIS TIME MUST BE BETWEEN 2049 AND 204799 SECONDS. SECONDS IS THE ONLY UNIT TO BE USED. THIS TIME IS ACCURATE TO ABOUT + OR - 3%. THE TIME READ WHEN 'E' IS HIT IS, HOWEVER, EXACT.
W	WRITE DATA	CAUSES COMPUTER TO PRINT OUT THE CONTENTS OF THE DATA FIELD IN THE FOLLOWING FORMAT. BIN NUMBER, TIME IN MICRO-SECONDS THAT THIS BIN CORRESPONDS TO, TOTAL SIGNAL PLUS NOISE (BEAM ON DATA FIELD), TOTAL NOISE (BEAM OFF DATA FIELD), SIGNAL (BEAM ON - BEAM OFF), STATISTICAL NOISE (SQUARE ROOT(S+N + N)), VELOCITY IN CM/SEC, AND FLUX AT THIS VELOCITY.

- ← COMMENT ALLOWS OPERATOR TO TYPE COMMENTS. HIT ' - ' (SHIFT O), COMPUTER WILL TYPE '/', TYPE ANYTHING YOU WANT. RETURN WILL CAUSE CARRIAGE RETURN LINE FEED AND WILL GET COMPUTER OUT OF COMMENT ROUTINE. TO TYPE FURTHER COMMENTS, OPERATOR MUST HIT ' - ' AGAIN.
- ↑ LOAD PARA. LOADS EXPERIMENTAL PARAMETERS. HIT ' ', (SHIFT N), COMPUTER WILL DO NOTHING, TYPE IN THE DELAY TIME IN MICRO-SECONDS (PLUS OR MINUS), TYPE SPACE, TYPE IN THE FLUX FUDGE FACTOR, (USUALLY 10000), TYPE RETURN. (WHERE RETURN AND SPACE ARE THE SINGLE KEYS ON THE KEYBOARD.)
- [ NS TELLS COMPUTER HOW MANY BINS YOU WANT IT TO SUM UP, (AVERAGE OVER). HIT '[ ', (SHIFT K), COMPUTER WILL PRINT "NS= ", TYPE IN AN INTEGER, TYPE RETURN.  
EXAMPLE: IF NS=3, THEN COMPUTER WILL, (WHEN TOLD), TYPE THE SUM OF THE CONTENTS OF BINS 1, 2, AND 3 AND CALL IT BIN NUMBER 3. CONTINUING, IT WILL SUM BINS 4, 5, AND 6 AND CALL IT BIN NUMBER 6. ETC. CURRENT DISCREPENCY. THE PROPER AVERAGE TIME FOR THE SUM OF THE FIRST 3 BINS WOULD BE HALF WAY THROUGH THE SECOND ONE. I. E. IF THE BIN TIME WERE 10  $\mu$ SECS, (AND THE DELAY TIME ZERO), THIS PROGRAM TYPES OUT THE TIME HALF-WAY THROUGH THE LAST BIN OF THE SUM, I. E. IN THIS EXAMPLE 25  $\mu$ SECS.

Table II

OP-CODE	INSTRUCTION
6170	LOAD COMMAND WORK
6171	SEND STATUS WORD TO ACC
6172	SEND COUNTING TIME CLOCK TO ACC
6173	LOAD COUNTING TIME CLOCK (CTC)
6174	LOAD BIN TIME GENERATOR
6175	LOAD MODE

DATA BIT	COMMAND	DATA BIT	STATUS
0		0	BIN TIME TOO FAST FLAG
1		1	TIME'S UP FLAG
2	CLEAR TIME'S UP FLAG	2	OVERFLOW FLAG
3	CLEAR OVERFLOW FLAG	3	
4	RESET CTC	4	
5	SET RUN	5	
6	SET STOP	6	
7	CLEAR BIN TIME TOO FAST	7	
8		8	
9		9	
10		10	
11		11	"GO" FLAG (1 = running, 0 = stopped)

corresponds to the detected ions somehow being delayed i. e. by the transit time through the quadrupole. Negative delay corresponds to the fast wheel pulse being "late" as in a mispositioned photo diode assembly or an externally applied delay of the fast wheel signal for purposes of "throwing away" the beginning portions of a TOF spectra. The latter process concerns the use of a delay generator between the fast wheel signal line driver and the computer.

The problem mentioned under "NS", i. e. that the printed accumulated bin time for an average over NS bins is not the proper average time, may be corrected by temporarily loading a new delay time = old delay time + NS x BIN TIME / 2. Example: if delay time setting is - 20, NS = 4, and BIN TIME = 20  $\mu$ secs then temporary new delay time, for this NS, is +20  $\mu$ secs.

In the WRITE DATA routine the last column is called the FLUX. This is a crude inversion of the time of flight data to give a velocity distribution. As shown in Eq. 1) the "FLUX" is equal to the measured intensity as a function of time multiplied by a Jacobian of  $t^2/d$ , which is also equal to  $d/v^2$ . Our detector, however, is not a flux detector; it is a number density detector because of the following. Normally the intensity would be given by the number of counts per sec per sq cm of detector area, a flux. However, the ionization probability, at low ionization efficiency, is inversely proportional to particle velocity because those molecules going faster spend less time in the detector and therefore have less probability of being ionized. Thus we measure flux  $\times 1/v$  or number density, No. /cm<sup>3</sup>. The last column, called FLUX, therefore prints out  $F \times$  intensity  $\times d/v$ , instead of divided by  $v^2$ .  $F$  is a fudge factor, normally  $10^4$ , to make the flux come out to reasonable numbers.

All of the above program fits into the 4K memory space of the computer with only a few scattered locations left. Even minor additions would require purchasing more memory. Such additions could include a program to punch data onto paper tape in a format that could be read by the Computation Center's computer, or possibly a program to time normalize angular distributions and plot them out on an X-Y recorder. Finally the existing hardware would be usable, without modification, with a pseudo random TOF technique but the program would have to be expanded to include the cross correlation (actually a relatively simple procedure).

Other TOF systems, described in references 9, 10 and 11, use interfaces similar to the one presented here.

#### APPENDIX I: Nozzle Geometry.

The geometry of the nozzle beam source, as modified for these experiments, is as follows. The nozzle has an orifice 0.02 cm in diameter and can be moved back and forth with respect to the skimmer to maximize the beam intensity.... the normal operating distance was 1.35 cm. The conical shaped skimmer has an orifice of 0.10 cm, is 2.76 cm from the center of the collision zone (CZ), and "empties" directly into the main chamber. The beam chopper is directly in front of the downstream side of the skimmer, about 1 cm from the CZ center. This geometry was calculated so as to not produce a viewing factor if the skimmer is assumed to act as a collimator. The viewing factor is simply the fraction of the total collision region that the detector can see as a function of the laboratory angle. The slit geometry of the detector (0.38 cm at entrance 4.44 cm from CZ and 0.3 cm at the ionizer entrance 18.44 cm from CZ) gives an umbra that subtends 0.4 cm at the CZ. If the collision zone, which is trapezoidal in shape, is larger than 0.4 cm then the detector will be

looking at varying volumes of reaction region as the lid is rotated causing an experimental bias in angular distribution measurements for certain angular regions over others. The easiest way to avoid this is to make sure that the largest dimension of the collision zone is less than 0.4 cm so that the detector is always viewing the whole collision zone (plus certain areas around it) at all angles.

If the skimmer was acting as a collimator, i.e. "casting" the standard umbra and penumbra "shadows", then there would be no viewing factor. However if the nozzle expansion has not frozen by the time it reaches the skimmer (i.e. the particles are still interacting with and deflecting each other) then the skimmer might act as a source giving a more divergent beam and possibly leading to a viewing factor. In fact, measurements made on the beam in this configuration, implied that this might partially be the case. Because of the geometry of the detector and because the detector rotates about the collision zone center and not about the beam radiant point the detection system can't see the beam beyond about  $+0.4^\circ$  (assuming the skimmer as the source). Therefore another method of measuring the beam profile was used: the background pressure in detector chamber one, which should be proportional to the amount of beam entering the detector, was monitored as a function of the lid angle which could be back calculated to the detector opening distance from the beam centerline. With the nozzle at 1.35 cm from the skimmer, and if the skimmer is assumed to collimate, then the beam at the detector opening should have an umbra of 1.07 and penumbra of 1.23 cm. Approximating this as a rectangle of width 1.15 cm and convoluting with the detector opening of 0.38 cm we get an expected FWHM of 1.53 cm. The measured distribution, with 150 torr in the nozzle, had a FWHM at the detector of 1.6 cm but contained a weak tail that went out to 2.7 cm (FW1/10M), so that the skimmer might be partially operating as a source.

In order to assure freedom from a viewing factor a beam collimator/deflector was spot welded to the face of the collimating chamber directly in front of the beam chopper. It consisted of a 0.5 cm wide horizontal strip of metal with a centrally located 1 cm diameter deflector containing a 0.23 cm wide by 0.38 cm high slot for the beam to pass through. The top and bottom of the deflector portion were angled away from the beam to deflect it above and below the region of the collision zone. For a proof of the absence of a viewing factor with this collimator installed, refer to figure 14 to which the following equations apply:

$$d_1 = 8.47(1.125/6.25) - .0125 = .140 \text{ cm}$$

$$d_2 = (2.76 + .115)(.12/1.81) - .05 = .140 \text{ cm}$$

Now we approximate the CZ by the dotted rectangle  $0.28 \times 0.28 \text{ cm}$ , an overestimate, and calculate its longest dimension, the dotted line, to be  $.39 \text{ cm}$  which is less than the  $0.4 \text{ cm}$  that the detector sees. Therefore, according to this calculation, there is no viewing factor. This was confirmed when the beam and detector geometries for both the Ba and Sn experiments were fed into a computer program, written by C. A. Mims<sup>12</sup>, that does a detailed calculation of the viewing factor taking all considerations into account. The factor was equal to 1.0 to within 0.002 for all angles. This was also confirmed experimentally by a repeat of the aforementioned beam profile measurement method.

## APPENDIX II Duty Cycle

Let  $S$  and  $B$  be the signal and background count rates respectively and let  $T_{\text{on}}$  and  $T_{\text{off}}$  be the time counted with the beam on and off. Then the absolute counts accumulated in the on channel is  $N_{\text{on}} = T_{\text{on}}(S+B)$  and off channel  $N_{\text{off}} = T_{\text{off}}(B)$ . Now the desired quantity is the total signal counts  $N_s$  given by the equation

$$N_s = N_{\text{on}}(T_{\text{on}} + T_{\text{off}})/2 T_{\text{on}} - N_{\text{off}}(T_{\text{on}} + T_{\text{off}})/2 T_{\text{off}}$$

$$(N_s = ((S+B)-B)(T_{on} + T_{off})/2 = S(T_{on} + T_{off})/2)$$

Now we make the condition that statistical noise in each of the two terms of  $N_s$  be equal so as to not put too much influence on one or the other. The statistical noise of the first term is  $\sqrt{N_{on}(T_{on} + T_{off})/2}$  since  $N_{on}$  is an absolute number of counts with, therefore, an error of  $\sqrt{N_{on}}$ , and  $(T_{on} + T_{off})/2$  is just a multiplying factor. Therefore we have the equation:

$$\sqrt{N_{on}(T_{on} + T_{off})/2} = \sqrt{N_{off}(T_{on} + T_{off})/2} \quad \text{or:}$$

$$\sqrt{T_{on}(S+B)/T_{on}} = \sqrt{T_{off}(B)/T_{off}} \quad \text{or:}$$

$$\sqrt{(S+B)/B} = \sqrt{T_{on}/T_{off}} \quad \text{so}$$

$$T_{on}/T_{off} = (S+B)/B \quad \text{or duty cycle } T_{on}/(T_{on} + T_{off}) = D$$

$$D = [(S+B)/B] / [(S+B)/B + 1] = (S+B)/(S+2B)$$

### APPENDIX III Circuit Diagrams

The detailed circuit diagrams for the TOF computer interface presented here are shown in figures 5 through 13. Only a brief description of each figure will be given. The circuits are built using mostly standard TTL circuits assembled on wire-wrap boards that plug into the PDP8/e Unibus. Not shown are the two D to A circuits that control the X-Y oscilloscope.

Fig. 5: Experiment control board including the GO flip flop (E30), the differentiator (E38), the delay generator (E26), the DMA ENABLE (E21), the DMA ADDRESS counters (E41 and E20) and the BTG too fast interrupt flag (E29). The differentiated slow wheel signal is gated into the delay generator by the GO flip-flop. The RUN command (data G valid) is loaded into E22 by IOTO and enables GO on the rising edge of SLOW WHEEL signal. The delayed signal (E26 pin 6 and 12) is passed to E18/E22 which is a glorified R/S flip flop. The rn signal enables (E21 pin 8) the DMA

enable (E21 pin 5) on the next falling edge of the TOF wheel pulse (E17 pin 10 from E39-6). This gates the BTG pulses (HAl-18) into the address counters (E41, E20). If the address counters time out before the next TOF pulse (256 cycles) the data breaking is stopped via the action of E21 pin 2 on the clear (pin 10). The BREAK REQUEST flag (E29) initiates DMA request via the action of the BTG (2, E25 pin 6). If another such request should come before the previous one is granted (CLR REQUEST) the BTG TOO FAST flag (E29 pin 3) will be set (on the coincidence of BRK REQUEST and BTG). The steering logic (E18 pins 5 and 6) is toggled by BTG.

Fig. 6: CYCLE COUNTERS. The cycle counters are loaded via IOTS. Upon being enable by the delayed slow wheel signal (E18 pin 3) the leading edges of TOF pulses start decrementing the cycle counters (E03, E04, E09). Upon time out the counters generate a pulse at E09 pin 13 which is passed through a one shot (E28) to generate the stop data pulse which disables the DMA ENABLE flip flop on the falling edge of the present TOF pulse (fig 6 E21). This pulse also presets the cycle counters to the value stored in the cycle count memory (E07, E02), and the process continues as described in the text of this chapter. The detailed timing diagram of this system is shown in figure 13. (The circuit works for any case of DSW coincident with FW).

Fig. 7: DATA COUNTERS. The signal counts from the PM discriminator (TTL level, negative going) are passed via the steering logic (C7-1, C7-2) to the A or B counters (A, B, C, 5 or A, B, C, 6). The 82591 is manufactured by Signetics Corp. The steering logic also directs which counters are to be read by the computer (C3; A, B, D3; A, B, D, 4; the 74126's are TRI-STATE buffers), and also which are to be

cleared by CLEAR REQUEST (B8). The TOF pulses (C7-6), from the TOF wheel discriminator (B8 pin 9) also clear the counters.

Fig. 8: BIN TIME GENERATOR (BTG). The bin time ( $\mu$ secs) is loaded by IOT4 into the 74174's. The crystal oscillator (E34) toggles the counters (E29, E25, E22) until their out matches the value held in the 74174's at which time the comparators (E28, E24, E20) bring the one shot's input up (E18 pin 2) causing a BTG pulse at (HAL-18) and resetting the counters for another cycle. (The counters are also reset by the TOF pulse (MA1-17))

Fig. 9: COUNTING TIME CLOCK (CTC). The binary mantissa of the desired count time is loaded by IOT3 from DATA lines 0 through 7 and this number is stored in 74174's and compared with the contents of counters much the same way the BTG works. In order to have a large range of count times, the CTC is designed to accept a binary exponent, in addition to the mantissa, loaded the same way from bits 7 through 11. This exponent is read by the MK5009 which is a MDS crystal oscillator and programmable divider. The MK5009 produces an out-put count at the rate of  $1\text{MHz} \div 2^n$  where n is the binary exponent. These output pulses (E37 pin 1) are counted by the binary counters (E33, E21, E08) and when the output of the last two (E21, E08) is equal to the stored mantissa the comparators trigger the TIME'S up interrupt flag (74107 pin 3). The count time can be read by IOT2... notice that while the "alarm" feature triggers off only the last two counters the read feature reads all three counters and gives the exact time.

Fig. 10: DMA CONTROL and Fig. 11: IOT CONTROL see the DEC manual "Small Computer Handbook" for an explanation of these circuits.

(Fig. 10 is correct.... DEC's figure contains an error.)

Fig. 13: The circuits for the small auxillary electronic devices are self explanatory. The following power supply voltages apply to fig. 13: NES29K: pin 10 = +6V, pin 3 = -6V, pin 9 = +SV; SN 75451P pin 8 = + 5V, pin 4 = GND. Use ground plane PC construction and bypass all power supplies with  $.05\mu F$  at 20 V ceramic capacitors.

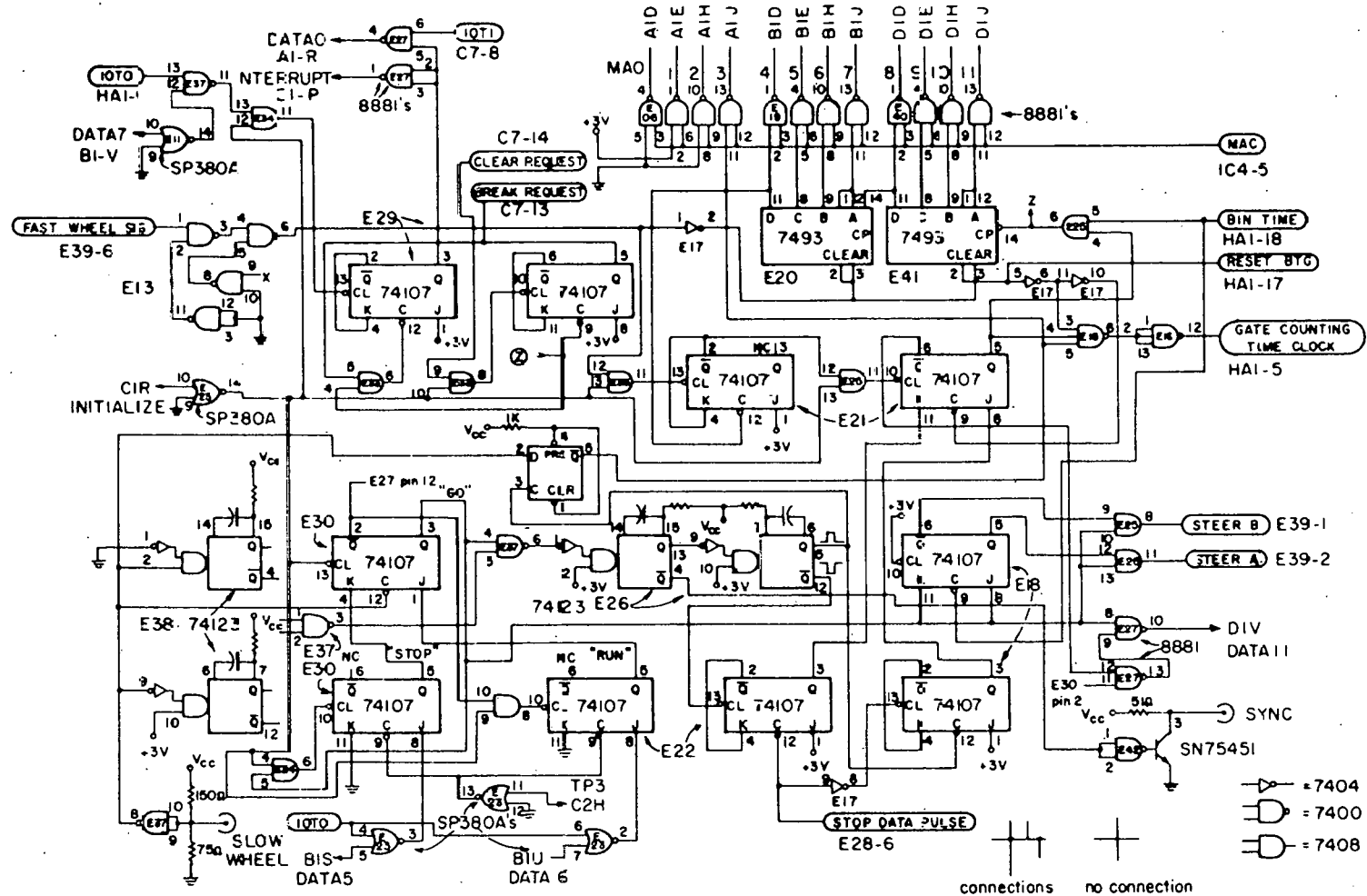


Fig. 5

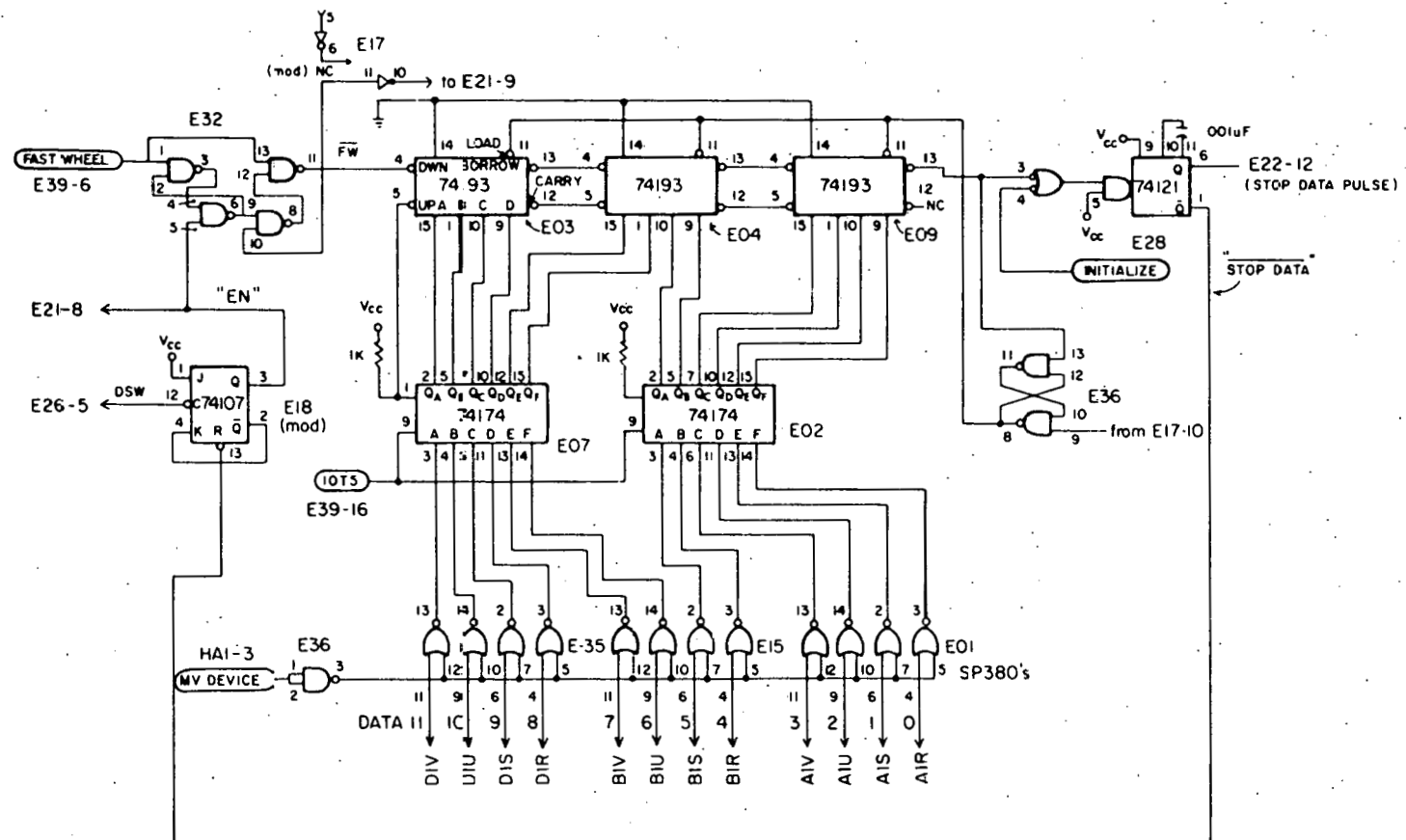


Fig. 6

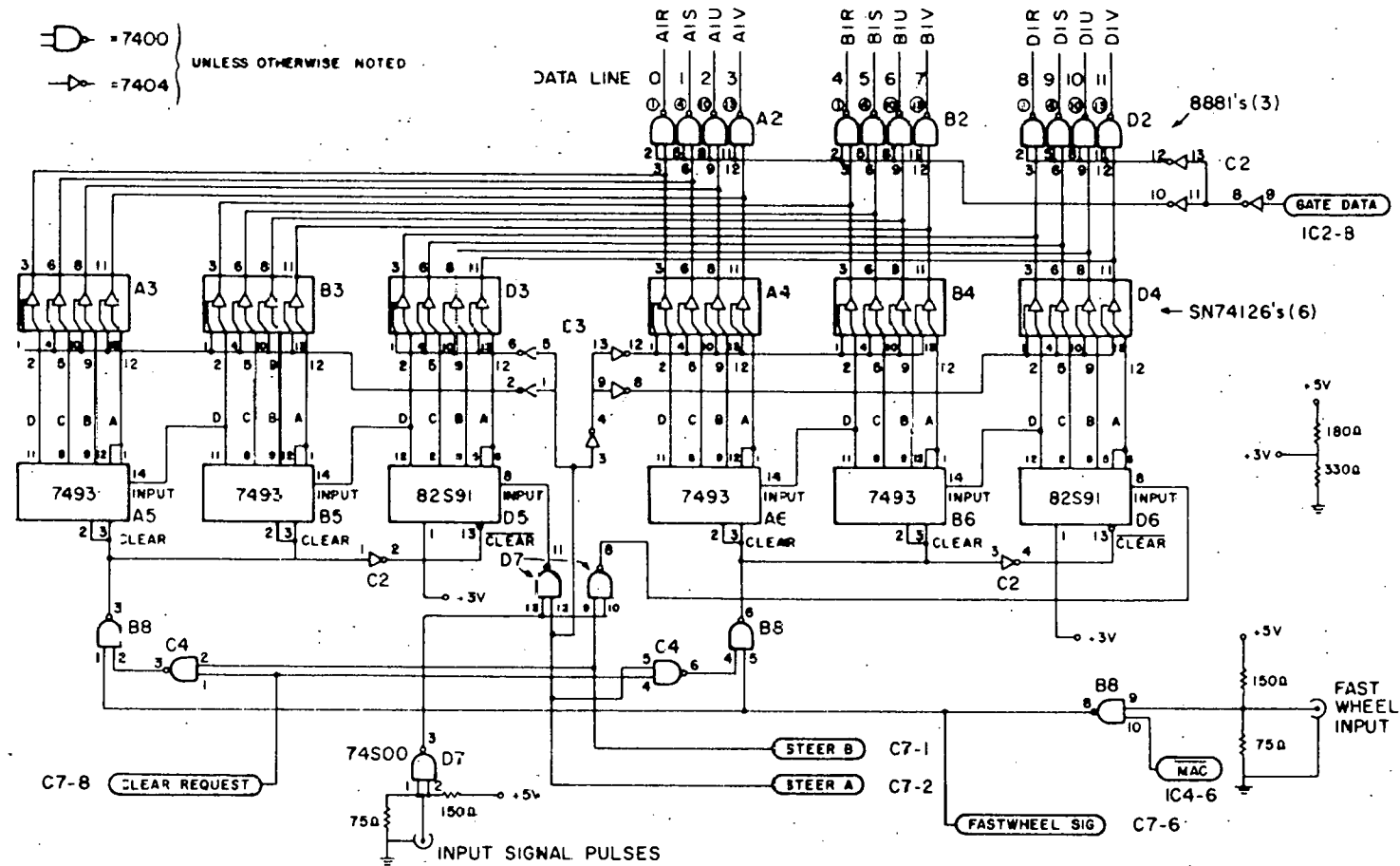


Fig. 7

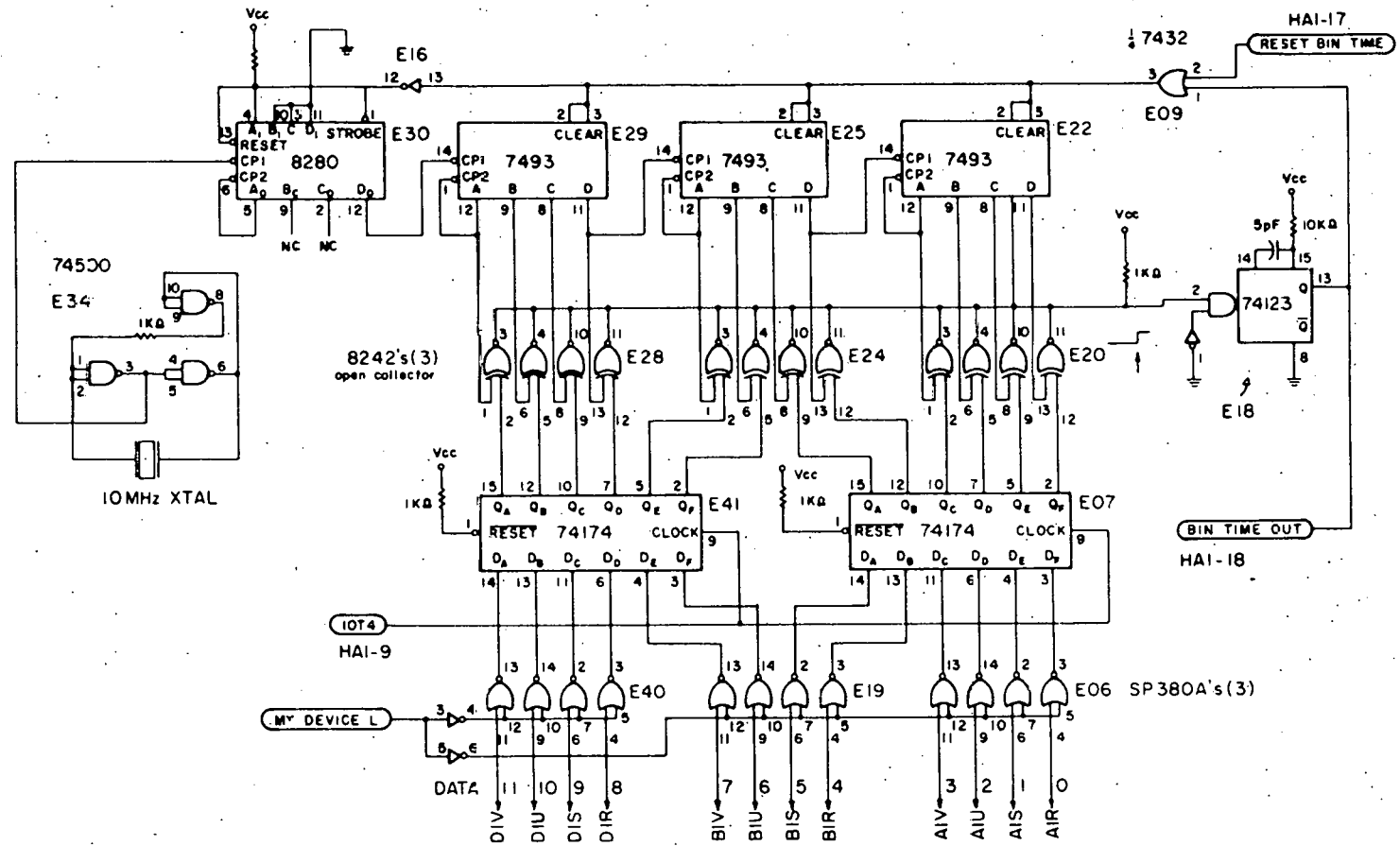


Fig. 8

(COUNTING TIME CLOCK)

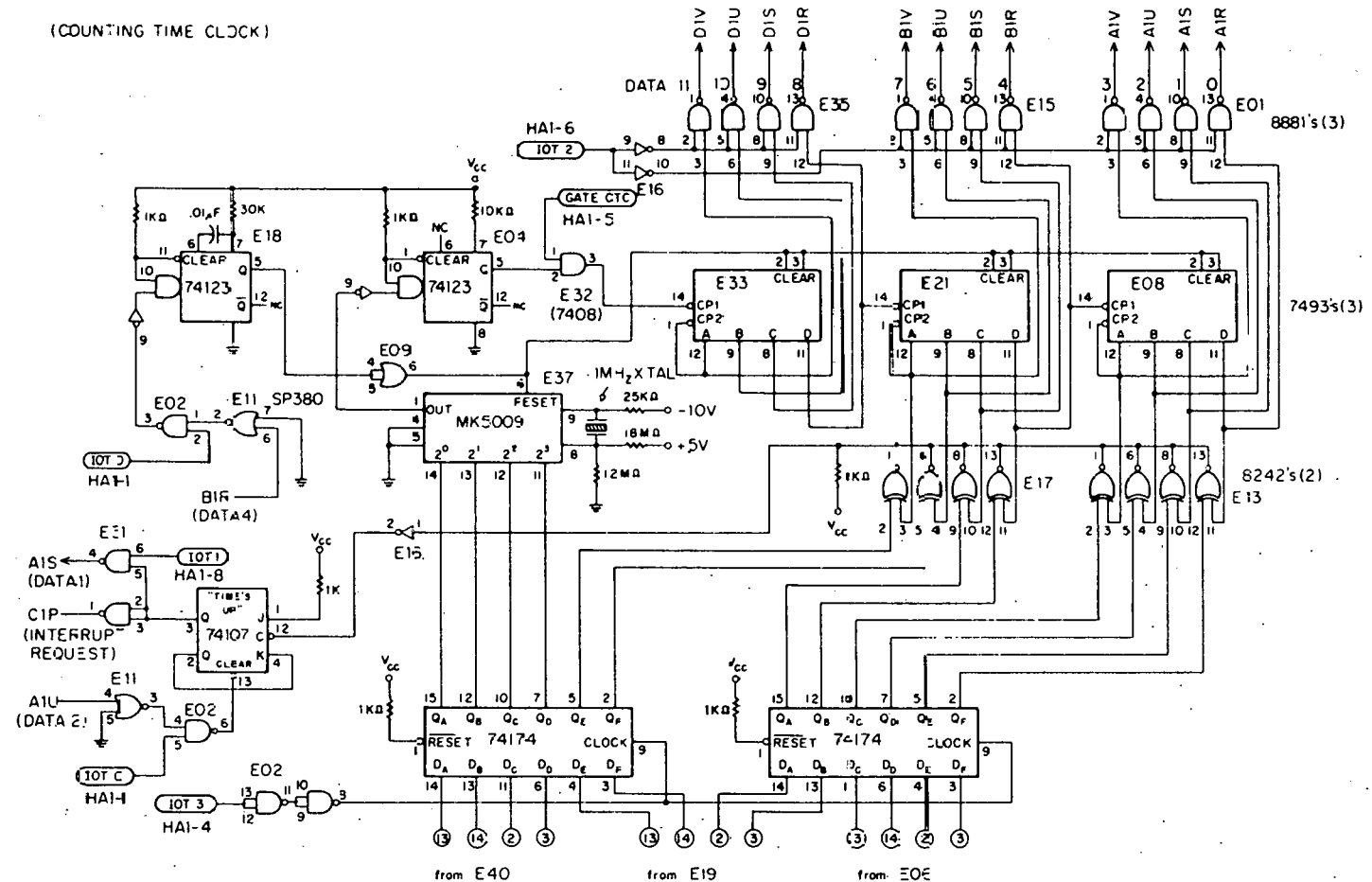


Fig. 9

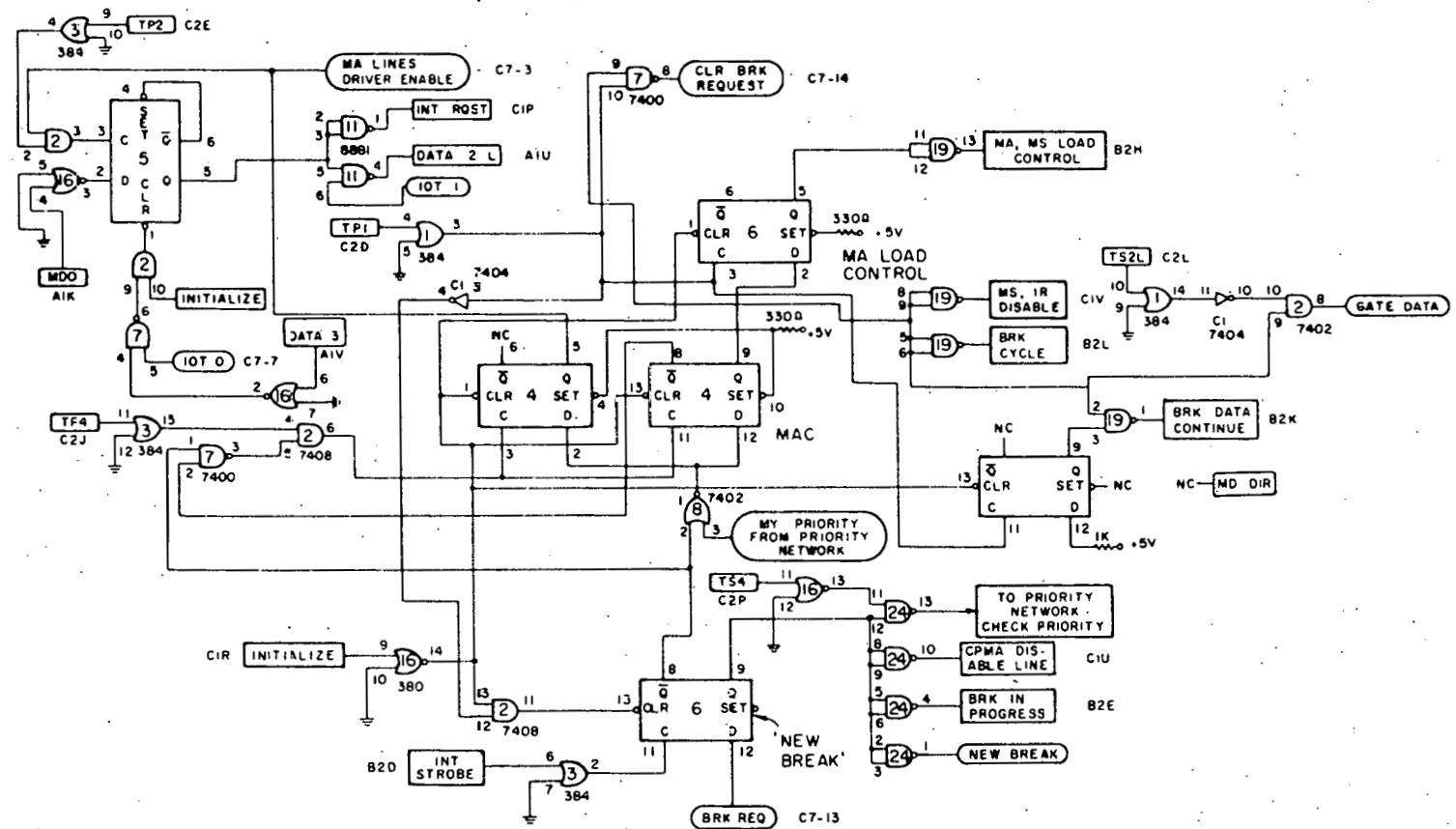
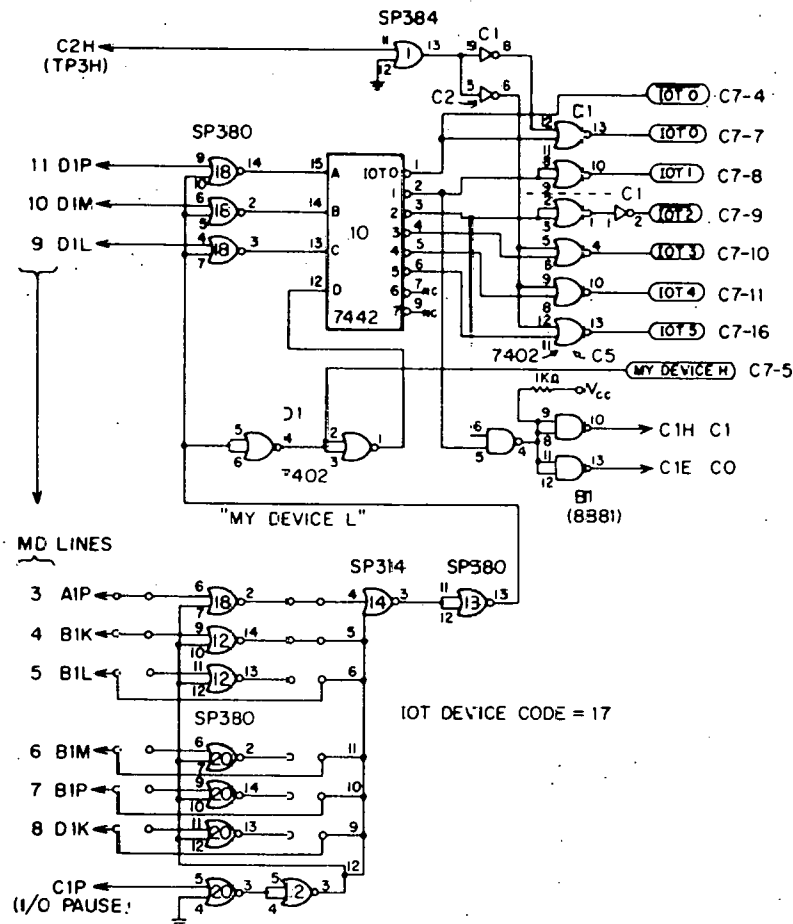


Fig. 10

## IoT CONTROL



## DATA BREAK PRIORITY NETWORK

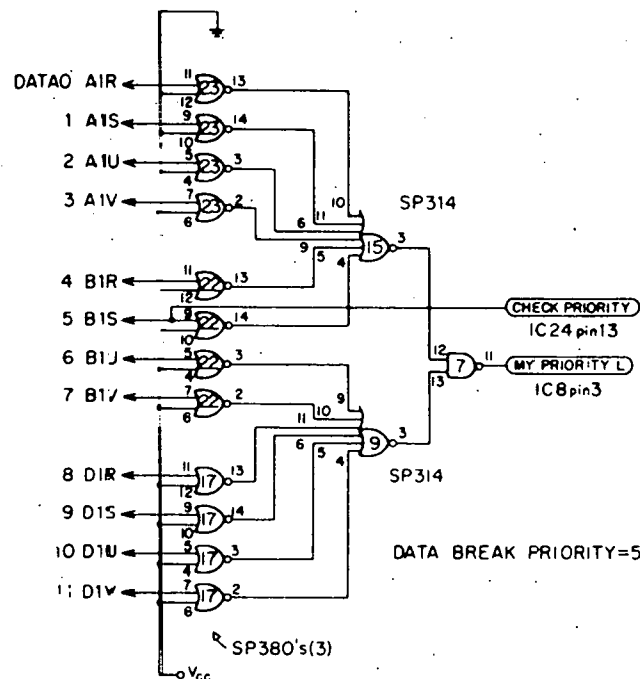
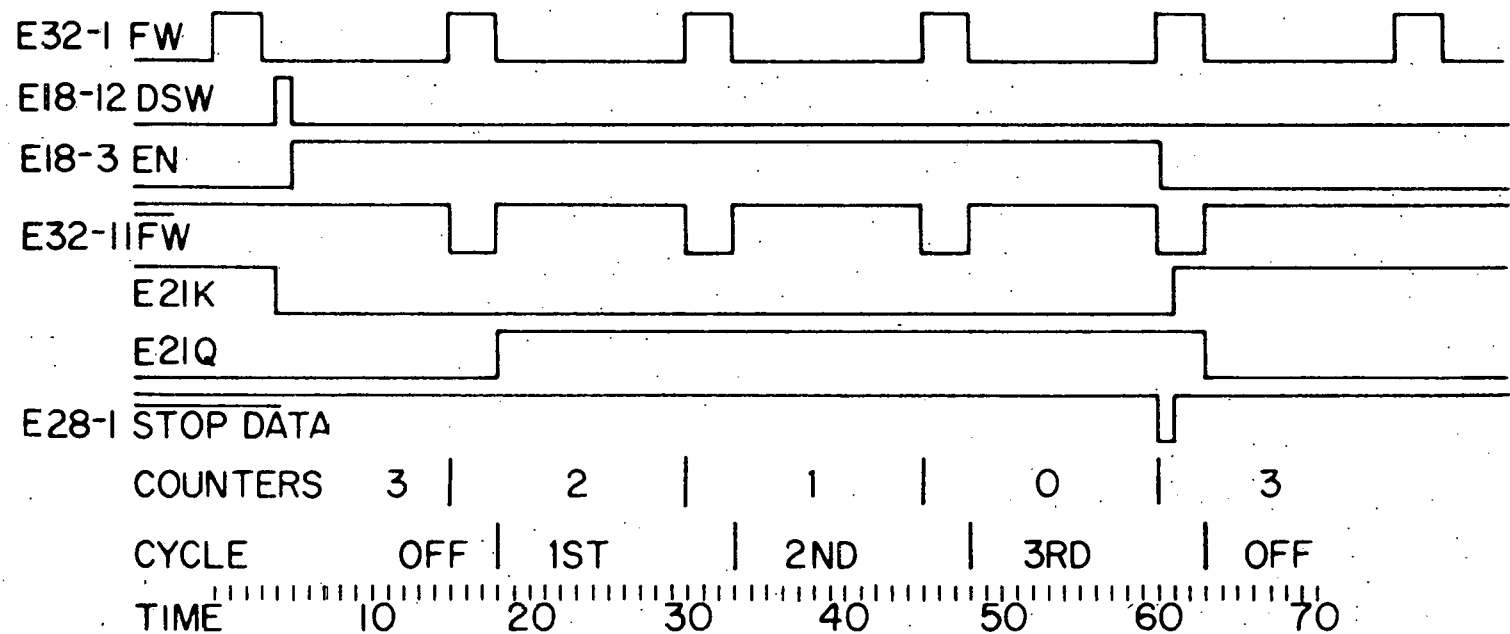


Fig. 11



-53-

CYCLE COUNTER TIMING DIAGRAM  
(NCYCLE=3)

Fig. 12

PM AND TOF DISCRIMINATORS  
(TOF VALUES IN PARENTHESSES)

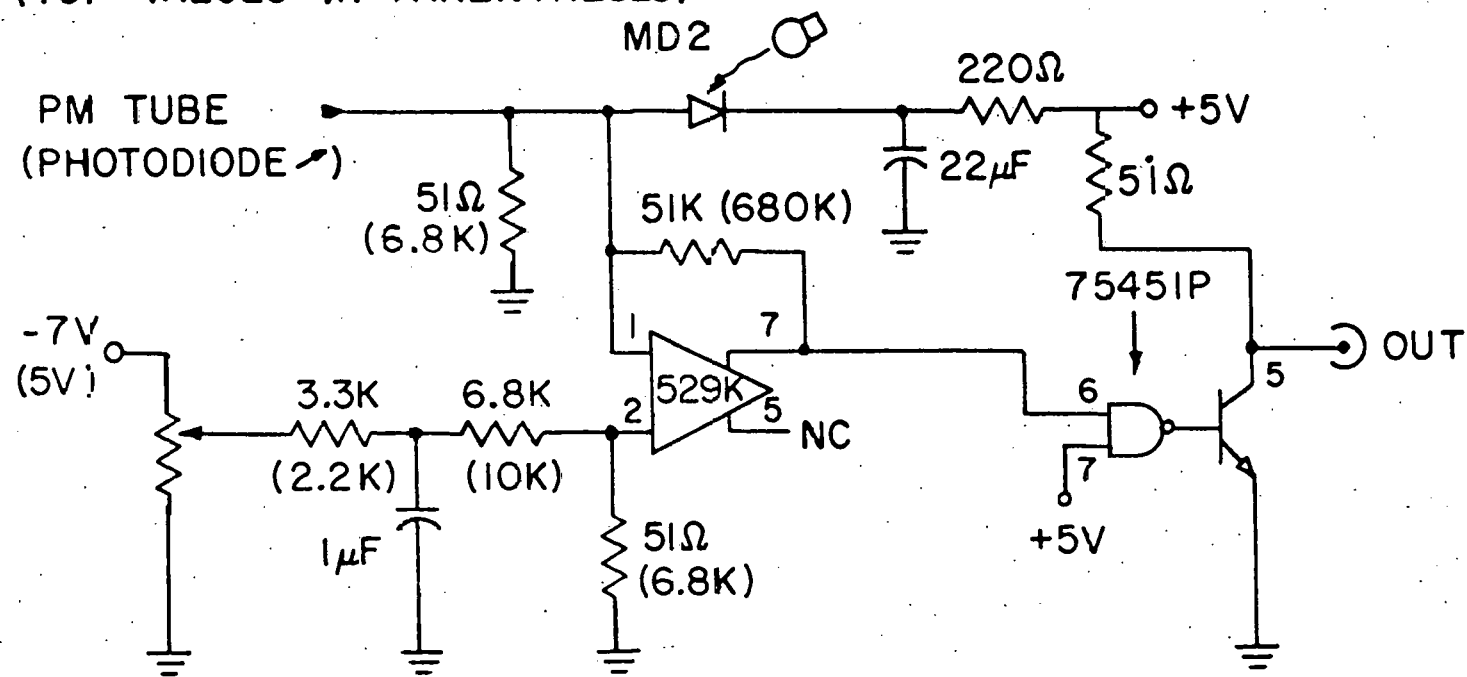
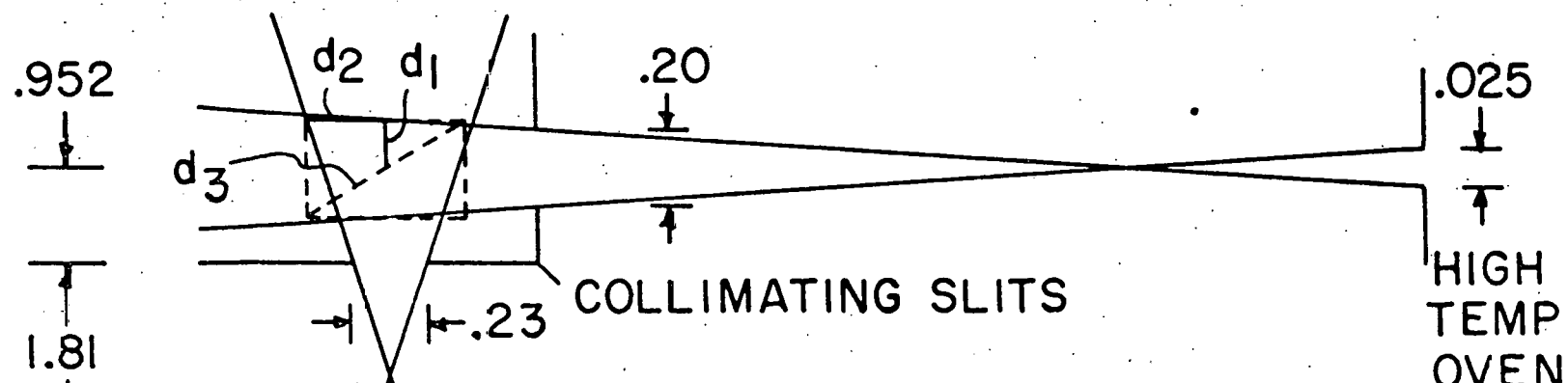


Fig. 13

## BEAM GEOMETRY (ALL DIMENSIONS IN cm)



፩፻፻፻

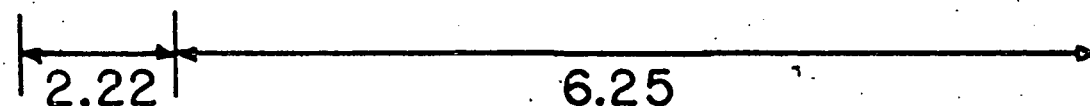


Fig. 14

References

1. Y. T. Lee, J. D. McDonald, P. R. LeBreton, D. R. Hershbach  
JCP 40, 1402 (1969).
2. R. Behrens, PhD thesis, Univ. of California at Berkeley.
3. A. Freedman, PhD thesis, Univ. of California at Berkeley.
4. Zircar - Union Carbide Corp.
5. R. Behrens, A. Freedman, R. Herm, T. Parr, Chem. Phys.  
Letters 36, 446 (1975).
6. G. O. Brink, Rev. Sci. Inst. 37, 857 (1966).
7. V. L. Hirsch, J. P. Aldridge, Rev. Sci. Inst. 42, 381 (1971).
8. K. Skold, Nuclear Inst. and Methods 63, 114 (1968).
9. R. Grice, Mol. Phys. 29, 1813.
10. J. P. McDonald, PhD thesis, Dept. of Chemistry, Harvard Univ.  
(1971).
11. J. D. McDonald, P. R. LeBreton, Y. T. Lee, D. R. Herschbach,  
JCP 56, 769 (1972).
12. C. A. Mims, PhD thesis, Univ. of California at Berkeley.
13. R. Behrens, A. Freedman, T. Parr, R. R. Herm, JCP, to be  
published Nov. 15.

COMPUTER PROGRAM LISTING

0000	0000	0000
0001	3030	DCA AC
0002	7004	RAL
0003	5010	JMP .+5
0004	0000	0000
0005	7400	7400
0006	7200	7200
0007	5600	5600
0010	3031	DCA L
0011	6171	6171 /READ STATUS WORD
0012	7100	CLL
0013	7010	RAR
0014	7440	SZA
0015	5100	JMP EXPS
0016	6031	KSF
0017	5022	JMP RESTOR
0020	5777	JMP KEYFLG
	7402	HLT
	7300	RESTOR, CLA CLL
	1031	TAD L
	7010	RAR
	1030	TAD AC
	6001	ION
	5400	JMP I O
0030	0000	AC, 0
	0000	L, 0
	0000	CRLF, 0
	7300	CLA CLL
	6046	TLS 1
	1076	TAD LF
	5063	JMP 63
	1000	FLAGR, 1000R /FLAGR=0, RUNNING
0063	6046	TLS /FLAGR≠0, STOPPED
	6041	TSF
	5064	JMP .-1
	7200	CLA
	1077	TAD CR
0070	6046	TLS
	6041	TSF
	5071	JMP .-1
	6042	TCF
	7300	CLA CLL
	5432	JMP 1 CRLF
	0212	LF, 212
	0215	CR, 215
	0100	*100
	7300	EXPS, CLA CLL
	6171	6171
	7006	RTL
	7004	RAL

0104	7420	SNL
	5710	JMP I 110
	5507	JMP I GRAND
	1000	1000
0110	1140	1140
		*111
0111	0000	SPACE, 0
	7300	CLA CLL
	1511	TAD I SPACE
	7041	CIA
	3126	DCA NSPCS
	1124	TAD TK240
	4525	JMS I ATLSX
0120	2126	ISZ NSPCS
	5116	JMP -3
	2111	ISZ SPACE
	5511	JMP I SPACE
	0240	240
	1242	ATLSX, 1242
	0000	NSPCS, 0
		*127
0127	4533	KILL, JMS I CLRK
0130	2000	2000
	3000	3000
	5144	JMP 144
	1546	CLRK, 1546
	0000	INPUT, 0
	7300	CLA CLL
	6046	TLS
	4405	JMS I 5
0140	6041	TSF
	5140	JMP -1
	6042	TCF
	5157	JMP FIX
	6001	ION
	5546	JMP I DISPZ
	1600	DISPZ, 1600
	0000	OUTPUT, 0
0150	7000	NOP
	6046	TLS
	4406	JMS I 6
	6041	TSF
	5153	JMP -1
	6042	TCF
	5547	JMP I OUTPUT
	7300	FIX, CLA CLL
0160	1171	TAD THIR
	1044	TAD 144
	3170	DCA NFIX
	1045	TAD 45
	7010	RAR
	2170	ISZ NFIX

00166	5164	JMP. -2
00167	5534	JMP I INPUT
00170	0000	NFIX, O
00171	7765	TMIR, (-13)
00172	0000	CTHOLD, O
00173	0000	O
00174	0000	O
00175	7600	ABSTOP, 7600
00176	0365	
*200		
00200	6002	IOF
00201	5602	IMP I 202
00202	1300	1300
*203		
00203	4134	JMS INPUT
00204	4407	JMS I 7
00205	6362	FPUT 362
00206	0000	FEXT
00207	5022	JMP RESTOR
*400		
00400	7300	KEYFLG, CLA CLL
00401	6636	KRB
00402	1223	TAD TZ0
00403	7510	SPA
00404	5777	JMP QM
00405	3221	DCA OFFSET
00406	1221	TAD OFFSET
00407	1224	TAD TF
00410	7700	SMA CLA
00411	5777	JMP QM
00412	1260	TAD SLIST
00413	1221	TAD OFFSET
00414	3222	DCA INSTRR
00415	1622	TAD I INSTRR
00416	3222	DCA INSTRR
00417	5622	JMP I INSTRR
00420	2402	HLT
00421	0000	OFFSET, 0000
00422	0000	INSTRR, 0000
00423	7477	TZ0, -301
00424	7741	TF, -37
*425		
00425	4631	STOPX, JMS SSTOP
00426	7240	CLA CMA
00427	3037	DCA FLAGR
00430	5022	JMP RESTOR
00431	7600	SSTOP
00432	1237	RNX, TAP K17
00433	6170	6170

00433	6170	6170
00434	7300	CLA CLL
00435	3037	DCA FLAGR
00436	5022	JMP RESTOR
00437	1700	147, 1700
00440	0000	
00441	00 00	
00442	7000	STATUS, NOP
00443	6171	6171
00444	7010	RAR
00445	7430	SZL
00446	5252	JMP 52
00447	4656	JMS I ATYPX
00450	5251	CMSTOP
00451	5254	JMP 54
00452	4656	JMS I ATYPX
00453	5245	CMRUN
00454	4032	JMS CRLF
00455	5022	JMS RESTOR
00456	1200	1200
00457	0005	ATYPX,

\*460

00460	0461	SLIST,	0461	/ADDR. 1ST PNTR.
00461	1063		NCYCLE	/A
00462	5000		BTX	/B
00463	1307		CONTX	/C
00464	1251		QM	/D
00465	5146		CTR	/E
00466	0532		FS	/F
00467	1251		QM	/G
00470	1251		QM	/H
00471	1251		QM	/I
00472	1251		QM	/J
00473	0127		KILL	/K
00474	1000		OVERF	/L
00475	1251		QM	/M
00476	1316		NBINX	/N
00477	1251		QM	/O
00500	1251		QM	/P
00501	0442		STATUS	/Q
00502	0432		RUNX	/R
00503	0425		STOPX	/S
00504	5142		QTLX	/T
00505	1353		SP	/U
00506	1360		DP	/V
00507	1000		WRITED	/W
00510	1341		SPN	/X
00511	1344		N	/Y
00512	1347		SIG	/Z
00513	1251		NS	/[
00514	1255		QM	/\
00515	1251		QM	/]
00516	1325		PAPAL	/↑
00517	1255		COMM	/←

00520	0000	O	1 ISZ XN
00521	7650	SNA CLA	1 IFF D. P.
00522	5720	JMP I 520	
00523	1731	TAD I 531	
00524	7710	SPA CLA	
00525	2730	ISZ I 530	1 ISZ XN
00528	2320	ISZ 520	
00527	5720	JMP I 520	1 RETURN
00530	1756	1756	1 AXN
00531	1545	1545	1 ASORD
00532	177.5	FS, TAD I AFI	1 FULL SCALE ROUTINE
00533	1364	TAD KF1	
00534	7041	CIA	
00535	3365	DCA KF2	
00536	4407	JMS I 7	1 EMTER F. P.
00537	5366	FGET KF3	
00540	0000	FEXT	1 EXIT F. P.
00541	4407	JMS I 7	1 ENTER F. P. (SEE 546)
00542	3371	FMULT KF4	
00543	7000	FNOR	
00544	0000	FEXT	
00545	2365	ISZ KF2	
00546	5341	JMP. -5	
00547	7300	CLA CLL	
00550	7000	NOP	
00551	4776	JMS I AF2	
00552	5255	CMFS	
00553	6040	SPF	
00554	7300	CLA CU	
00555	1374	TAD FF8	
00556	3062	DCA 62	
00557	4406	JMS OUTPUT	
00560	6041	TSF	
00561	5360	JMP. -1	
00562	4032	JMS CRLF	
00563	5022	JMP RESTOR	
00564	0000	KF1,	6
00565	0000	JF2,	0
00566	0007	K.F.,	FLTG 178
00567	2000		
00570	0000		
00571	0001	KF4,	FLTG 2
00572	2000		
00573	0000		
00574	0010	KF8,	10
00575	1762	AF1,	1762
00576	1200	AF2,	1200
00577	1251	QM,	1251
00600	4756	WRITED,	JMS SSTOP
00601	4487		JMS I 7 /SETS STOP

00602	5772	FGET
00603	6771	FPUT FBINN
00604	0000	FEXT
00605	5210	JMP 13
00606	5210	JMS 32 /EXPECTS CRLF TO BE AT 0032
00607	4032	JMS 32
00610	5611	JMP 1611
00611	1371	1371
00612	0260	260
00613	4753	JMS I ATYPX /EXPECTS TYPX TO BE AT 1200
00614	5300	CMBIN
00615	4111	JMS SPACE
00616	0005	5
00617	4753	JMS I ATYPX
00620	5302	CMTIME
00621	4111	JMS SPACE
00622	0006	6
00623	4753	JMS I ATYPX
00624	5305	CMSPEN
00625	4111	JMS SPACE
00628	0010	10
00627	4753	JMS I ATYPX
00630	5307	CMN
00631	7300	CLACLL
00632	3045	DCA95
00633	3046	DCA96
00634	4407	JMS I 7
00635	6779	FPUT FSF
00636	6773	FPUT FSFV
00637	0000	FEXT
00640	7300	CLA CLL
00641	1376	TAD (3002)
00642	3354	DCA BINNUM
00643	1375	TAD (4002)
00644	3355	DCA ZINNUM
00645	7000	NOP
00646	7300	CLA CU
00647	3045	DCA 95
00650	3046	DCA 46
00651	4407	JMS I 7
00652	6767	FPUT SPNR EG
00653	6766	FPUT NR EG
00654	0000	FEXT
00655	7300	CLA CLL
00656	1754	TAD I BINNUM
00657	3046	DCA 46
00660	2354	I SZ BINNUM
00661	1754	TAD I BINNUM
00662	3045	DCA 45
00663	1370	TAD (27)
00664	3044	DCA 44
00665	4407	JMS 17
00666	1767	FADD SPNR EG
00667	6767	FPUT SPNR EG /LOADS S+N REG
00670	0000	FEXT
00671	1755	TAD I ZINNUM
00672	3046	DCA 46
00673	2355	I SZ ZINNUM
00674	1755	TAD I ZINNUM
00675	3045	DCA 45
00676	1370	TAD (27)
00677	3044	DC A44

00701	1760	FADD NREG	
00702	6766	FPUT NREG	/LOADS N REG
00703	5767	FGET SPNREG	
00704	2766	FSUB NREG	
00705	6765	FPUT SREG	/LOADS SIG (DIFF) REG
00706	57 71	FGET FBINN	
00707	3764	FMPY FTWO	
00710	2772	FSUB FONE	
00711	3763	FMPY FBINT	
00712	4764	FDIV FTWO	
00713	2762	FSUB FDT	
00714	6761	FPUT FTIME	/TIME=BINTIME*(2BIN#-1)/2 - DEL
00715	0000	FEXT	
00716	5612	JMP I 612	
00717	4760	JMS TYPE	
00720	0003	3	
00721	4407	JMS I 7	
00722	57 61	FGET FTIME	
00723	0000	FEXT	
00724	4760	JMS TYPE	
00725	0006	6	
00726	4407	JMS I 7	
00727	5767	FGET SPNREG	
00730	0000	FEXT	
00731	4760	JMS TYPE	
00732	0007	7	
00733	4407	JMS I 7	
00734	57 66	FGET NREG	
00735	0000	FEXT	
00736	47 60	JMS TYPE	
00737	0007	7	
00740	4407	JMS I 7	
00741	57 65	FGET SREG	
00742	0000	FEXT	
00743	47 60	JMS TYPE	
00744	0007	7	
00745	4407	JMS I 7	
00746	5767	FGET SPNREG	
00747	1766	FADD NREG	
00750	0002	SQROOT	
00751	0000	FEXT	
00752	5757	JMP 210	
00753	1200	ATYPX, 1200	
00754	0000	BINNUM, 0	
00755	0000	ZINNUM, 0	
00756	7600		
00757	0210		
00760	0302		
00761	0332		
00762	0351		
00763	0346		
00764	0340		
00765	0327		
00766	0324		
00767	0321		
00770	0021		
00771	0335		
00772	0343		
00773	0316		
00774	0313		

00777 0040 \*210

00210 4302 JMS TYPE  
 00211 0004 4  
 00212 5613 JMS I 213  
 00213 0233 233  
 00214 3357 FMPY FMILL  
 00215 4332 FDIV FTIME  
 00216 6321 FPUT SPNREG  
 00217 0000 FEXT  
 00220 4302 JMS TYPE  
 00221 0007 7  
 00222 4407 JMS I 7  
 00223 5327 FGET SREG  
 00224 3354 FMPY FDIST  
 00225 4321 FDIV SPNREG  
 00226 6324 FPUT NREG  
 00227 3362 FMPY FTTHOU  
 00230 0000 FEXT  
 00231 4302 JMS TYPE  
 00232 0007 7  
 00233 4407 JMS I 7  
 00234 5324 FGET NREG  
 00235 1313 FADD FSF  
 00236 6313 FPUT FSF  
 00237 5324 FGET NREG  
 00240 3321 FMPY SPNREG  
 00241 1316 FADD FSFV  
 00242 6316 FPUT FSFV  
 00243 5335 FGET FBINN  
 00244 1343 FADD FONE  
 00245 6335 FPUT FBINN  
 00246 2365 FSUB FNBBINS  
 00247 0000 FEXT  
 00250 4032 JMS CRLF  
 00251 1045 TAD 45  
 00252 7550 SPA SNA  
 00253 5274 TMP KRYQ  
 00254 5022 JMP RESTOR  
 00255 4032 JMS CRLF  
 00256 4032 JMS CRLF  
 00257 5022 JMP RESTOR  
 00260 2111 ISZ BINNUM  
 00261 2776 ISZ ZINNUM  
 00262 2370 ISZ NSP  
 00263 5773 JMP I 373  
 00264 7300 CLA CLL  
 00265 1271 TAD NBIND  
 00266 7041 CIA  
 00267 3370 PCA NSP  
 00270 4407 JMS I 7  
 00271 5335 FGET FBINN  
 00272 0000 FEXT  
 00273 5772 JMP I 372  
 00274 6031 KEYQ, KSF  
 00275 5774 JMP RETUR  
 00276 6030 KCF  
 00277 4775 JMS TYPX  
 00300 5351 CMTERM  
 00301 5255 JMP 255  
 00302 0000 TYPE, 0  
 00303 6046 T.I.S

-64-

/FOR FLUX 212=4407  
 /AND 213-5354

/SPNREG NOW USED TO HOLD VELOCITY

/NREG NOW USED FOR FLUX

00777 0040

\*210

-65-

00210	4302	JMS TYPE
00211	0004	4
00212	5613	JMS I 213 / FOR FLUX 212 = .4407
00213	0233	233 1 AND 213 = 5354
00214	3357	FMPY FMILL
00215	4332	FDIV FTIME
00216	6321	FPUT SPNREG / SPNREG NOW USED TO HOLD VELOCITY
00217	0000	FEXT
00220	4302	JMS TYPE
00221	0007	7
00222	4407	JMS I 7
00223	5327	FGET SREG
00224	3354	FMPY FDIST
00225	4321	FDIV SPNREG
00226	6324	FPUT NREG /NREG NOW USED FOR FLUX
00227	3362	FMPY FTTHOU
00230	0000	FEXT
00231	4302	JMS TYPE
00232	0007	7
00233	4407	JMS I 7
00234	5324	FGET NREG
00235	1313	FADD FSF
00236	6313	FPUT FSF
00237	5324	FGET NREG
00240	3321	FMPY SPNREG
00241	1316	FADD FSFV
00242	6316	FPUT FSFV
00243	5335	FGET FBINN
00244	1343	FADD FONE
00245	6335	FPUT FBINN
00246	2365	FSUB FNBINS
00247	0000	FEXT
00250	4032	JMS CRLF
00251	1045	TAD 45
00252	7550	SPA SNA
00253	5274	JMP KEYQ
00254	5022	JMP RESTOR
00255	4032	JMS CRLF
00256	4032	JMS CRLF
00257	5022	JMP RESTOR
00260	2777	ISZ BINNUM
00261	2776	ISZ ZINNUM
00262	2370	ISZ NSP
00263	5773	JMP I 373
00264	7300	CLA CLL
00265	1271	TAD NBIND
00266	7041	CLA
00267	3370	PCA NSP.
00270	4407	JMS I 7
00271	5335	FGET FBINN
00272	0000	FEXT
00273	5772	JMP I 372
00274	6031	KEYQ, KSF
00275	5774	JMP RETUR
00276	6030	KCF
00277	4775	JMS TYPX
00300	5351	CMTERM
00301	5255	JMP 255
00302	0000	TYPE, O
00303	6046	TLS
00304	1702	TAD I TYPE

00306	4406	JMS I 6
00307	4111	JMS SPACE
00310	0003	3
00311	2302	ISZ TYPE
00312	5702	JMP I TYPE

00313	0000	FSF,      FLTG 0
00314	0000	
00315	0000	
00316	0000	FSFV,      FLTG 0
00317	0000	
00320	0000	
00321	0000	SPNREG,      FLTG 0
00322	0000	
00323	0000	
00324	0000	NREG,      FLTG 0
00325	0000	
00326	0000	
00327	0000	SREC,      FLTG 0
00330	0000	
00331	0000	
00332	0000	FTIME,      FLTG 0
00333	0000	
00334	0000	
00335	0000	FBINN,      FLTG 0
00336	0000	
00337	0000	
00340	0002	FTWO,      FLTG 2
00341	2000	
00342	0000	
00343	0001	FONE,      FLTG 1
00344	2000	
00345	0000	
00346	0007	FBINT,      FLTG 100
00347	3100	
00350	0000	
00351	0000	FDT,      FLTG 0
00352	0000	
00353	0000	
00354	0004	FDIST,      FLTG 10
00355	2400	
00356	0000	
00357	0024	FMILL,      FLTG 1.0E06
00360	3641	
00361	1000	
00362	0016	FTTHOU,      FLTG 1.0E04
00363	2342	
00364	0000	
00365	0006	FNBINS,      FLTG 32
00366	2000	
00367	0000	
370	7777	
371	1764	
372	0717	
373	5334	

00375 1200  
00376 0755  
00377 0754  
- \*5300  
05300 0211 CMBIN, TEXT "BI  
05301 1600 N"  
05302 2411 CMTIME, TEXT "TI  
05303 1505 ME  
05304 0000 "  
05305 2353 CMSPN, TEXT "S+  
05306 1600 N"  
05307 1600 CMN, TEXT 'N  
05310 4040  
05311 4040  
05312 4040  
05313 0411 CMD  
05314 0606 FF  
05315 4040  
05316 4040  
05317 2321 SQ  
05320 4022 R  
05321 2440 T  
05322 4026 V  
05323 0514 EL  
05324 1703 OC  
05325 1124 IT  
05326 3140 Y  
05327 4040  
05330 4006 F  
05331 1425 LU  
05332 3037 X "  
05333 3700 "  
05334 4407 JMS I 7  
05335 5742 FGET FBINN  
05336 1743 FADD FONE  
05337 6742 FPUT FBINN  
05340 0000 FEXT  
05341 5744 JMP RETWED  
05342 0335 FBINN, 335  
05343 0343 FONE, 343  
05344 0655 RETWED, 655  
05345 0000 0  
05346 0000 0  
05347 0000 0  
05350 0000 0  
05351 4024 CMTERM, TEXT " T  
05352 0522 ER  
05353 1511 MI  
05354 1601 NA  
05355 2405 TE  
05356 0400 D "  
\*1000  
01000 7300 OVERF, CLA CLL  
01001 1377 TAD (40)  
01002 6170 LCW

/ STOP EXP.

01005	3333	DCA AOV
01006	1330	TAD BIOV
01007	3334	DCA BOV
01010	3336	DCA FLGOV
01011	6171	RSW
01012	7010	RAR
01013	7430	SZL
01014	5211	JMP. -3
01015	7300	CLA CLL
01016	1332 GOAUNO,	TAD KOV2
01017	6170	LSW
01020	7000	NOP
01021	7300 RETOV,	CLA CLL
01022	2333	ISZ AOV
01023	2334	ISZ BOV
01024	1734	TAD I BOV
01025	1733	TAD I AOV
01026	3734	DCA I BOV
01027	3733	DCA I AOV
01030	7004	RAL
01031	2334	ISZ BOV
01033	1734	TAD I DOV
01033	7430	SZL
01034	4255	JMS TYP0VR
01035	7510	SPA
01036	2336	ISZ FLGOV
01037	3734	DCA I BOV
01040	5243	JMP 1 to 43
01041	1337	TAD KOV1
01042	5314	JMP 1114
01043	1330	TAD BIOV
01044	7041	CIA
01045	1333	TAD AOV
01046	7710	SPA CLA
01047	5221	JMP RETOV
01050	5307	JMP GOBCK
01051	1037	TAD FLAGR
01052	7440	SZA
01053	5727	JMP 11127
01054	5241	JMP 1041
01055	0000 TYP0VR,	0
01056	7300	CLA CLL
01057	7604	LAS
01060	7010	RAR
01061	7430	SZL
01062	5655	JMP I TYP0VR
01063	4032	JMS CRLF
01064	7900	NOP
LG 01065	4776	JMS TYPX
01066	5233	CMOVER
01067	1326	TAD AIOV
01070	7041	CIA
01071	1333	TAD AOV
01072	3045	DCA 45
01073	3046	DCA 46
01074	1375	TAD (13)
01075	3044	DCA 44
01076	4407	JMS I 7
01077	7000	FNOR
01100	0000	FEXT
01101	7240	CLA CMA
01102	3055	DCA 55
01103	1374	TAD (3)

01104	3062	DCA 62
01105	4547	JMS OUTPUT
01106	5655	JMP I TYPOVR
01107	7300	GOBCK,
01110	1336	CLA CLL
01111	7440	TAD FLGOV
01112	5317	SZA
01113	5251	JMP +5
01114	6170	JMP 1051
01115	5022	6170
01116	7600	JMP RESTOR
01117	4716	ASTOP
01120	4032	JMS SSTOP
LG 01121	4776	JMS CRLF
	5200	JMSTYPX
	7201	CMFULL
	3037	CLA IAC
	5022	DCA FLAGR
	1777	JMP RESTOR
	AIOV,	1777
01127	0600	0600
01130	2777	BIOV,
01131	0000	2777
01132	0440	0
01133	0000	440
01134	AOV,	0
01135	0000	0
01136	BOV,	0
01137	0000	0
01138	NOV,	0
01139	0500	FLGOV,
01140	0500	KOVI,
01141	4575	0500
01142	4575	JMS I 175
01143	6171	JMS I 175
01144	7004	RSW
01145	7004	RAL
01146	7430	SZL
01147	5361	JMP 1153
01148	5361	RAL
01149	7430	SZL
01150	7402	JMP 1161
01151	5022	HLT
01152	5022	JMP RESTOR
01153	4767	JMS TYPX
01154	5263	CMBTG
01155	4032	JMS CRLF
01156	1370	TAD KE20
01157	6170	LSW

1160	5022	JMP RESTOR
1160	5022	JMP RESTOR
1161	4767	JMS TYPX
1162	5272	CMTIME
1163	4032	JMS CRLF
1164	1371	TAD KEIK
1165	6170	LSW
1166	5372	JMP 1172
1167	1200	
1170	0020	
1170	0020 KEZO,	20
1171	1000 KEIK,	1000
1172	3037	DCA FLAGR
1173	5022	JMP RESTOR
01174	0003	
01175	0013	
01176	1200	
01177	0400	
	*1200	
01200	0000 TYPX,	0
01201	7300	CLA CLL
01202	1600	TAD I TYPX
01203	3214	DCA TYPNT
01204	2200	ISZ TYPX
01205	1614 TYPXI,	TAD I TYPNT
01206	7002	
01207	4215	JMS TYPY
01210	1614	TAD I TYPNT
01211	2214	ISZ TYPNT
01212	4215	JMS TYPY
01213	5205	JMP TYPX1
01214	0000 TYPNT,	0
01215	0000 TYPY,	0
01216	0234	AND TK77
01217	7450	SNA
01220	5600	JMP I TYPX
01221	1235	TAD TKM37
01222	7440	SZA
01223	522u	JMP TYPY1
01224	1236	TAD TK215
01225	4242	JMS TLSX
01226	1231	TAD TKM125
01227	7510 TYPY1,	SPA
01230	1240	TAD TK100
01231	1241	TAD TK237
01232	4242	JMS TLSX
01233	5615	JMP I TYPY
01234	0077 TK77,	77
01235	7741 TKM37,	-37
01236	0215 TK215,	215
01237	7653 TKM125,	-125
01240	0100 TK100,	100
01241	0237 TK237,	237

01243	6046	TLS
01244	6041	TSF
01245	5244	JMP
01246	6042	TCF
01247	7200	CLA
01250	5642	JMP I TLSX
01251	4654	JMS I QMK
01252	7300	CLA CLL
01253	5022	JMP RESTOR
01254	0032	CRLF

\*QMK+1

01255	7300	COMM,	CLA CLL
01256	1275		TAD TK334
01257	4242		JMS TLSX
01260	6031		KSF
01261	5260		JMP -1
01262	6036		KRB
01263	7041		CIA
01264	1236		TAD TK215
01265	7440		SZA
01266	5271		JMP ECHO
01267	4032		JMS CRLF
01270	5022		JMP RESTOR
01271	7041	ECHO,	CIA
01272	1236		TAD TK215
01273	4242		JMS TLSX
01274	5260		JMP COMM+3
01275	0257	TK257	257

\*1400

01400	0000	DPDADD, 0	
01401	7300	CLA CLL	
01402	1345	TAD SORD	/S.P. DATA MUST BE IN N
01403	7710	SPA CLA	/D.P. DATA MUST BE IN M
01404	1377	TAD (400)	
01405	1377	TAD (400)	
01406	1776	TAD XN	/ADDS PRESENT DATA
01407	3261	DCA YN	/TO HOLDING REG (ALSDSN ETC.)
01410	1776	TAD XN	
01411	3260	DCA PADD	
01412	1373	TAD AA00I	
01413	3257	DCA AADD	
01414	7100	RETADD, CLL	
01415	1660	TAD I PADD	
01416	1657	TAD I AADD	
01417	3657	DCA I AADD	
01420	1345	TAD SORD	
01421	7700	SMA CLA	
01422	5227	JMP .+5	
01423	7004	RAL	
01424	2260	ISZ PADD	
01425	1660	TAD I PADD	
01426	7410	SKP	
01427	7004	RAL	
01430	2257	ISZ AADD	
01431	1657	TAD I AADD	
01432	3657	DCA I AADD	
01433	7004	HAL	
01434	2257	ISZ AADD	
01435	1657	TAD I AADD	
01436	3657	DCA I AADD	
01437	1257	TAD AADD	
01440	7041	CIA	
01441	1371	TAD AA00I3	
01442	4770	JMS I 1570	
01443	5600	JMP I DPDADD	
01444	1361	TAD YN	
01445	3260	DCA PADD	
01446	1372	TAD AA00I2	
01447	3257	DCA AADD	
01450	5214	JMP RETADD	
01451	0000	ALSDSN, 0	
01452	0000	AMSDSN, 0	
01453	0000	AHSDSN, 0	
01454	0000	ALSDN, 0	
01455	0000	AMSDN, 0	
01456	0000	AHSDN, 0	
01457	0000	AADD, 0	
01460	0000	PADD, 0	
01461	0000	YN, 0	
01462	0000	DPDSUB, 0	/TAKES SUM(S+N)-SUM(N) AND PUTS /IT IN LSDH ETC. ('TRIPLE PREC')
01463	7300	CLA CLL	
01464	1254	TAD ALSDN	
01465	7041	CIA	
01466	1251	TAD ALSDSN	
01467	3307	DCA LSDH	
01470	7004	RAL	
01471	3312	DCA KEEPD	
01472	1255	TAD AMSDN	
01473	7040	CMA	
01474	1252	TAD AMSDSN	
01475	1312	TAD KEEPD	

01477	7004	RAL	
01500	3312	DCA KEEPD	
01501	1256	TAD AHSDN	
01502	7040	CMA	
01503	1253	TAD AHSDSN	
01504	1312	TAD KEEPD	
01505	3311	DCA HSDH	
01506	5662	JMP I DPDSUB	
01507	0000	LSDH, 0	
01510	0000	MSDH, 0	
01511	0000	HSDH, 0	
01512	0000	KEEPD, 0	
01513	7200	CHECKD, CLA	/CHECKS WHETHER YOU WANT TO DIS
01514	1344	TAD SORN	/S+N, N, OR S+N-N=S AND LOADS L
01515	7510	SPA	/ACCORDINGLY
01516	5325	JMP NOISE	
01517	7640	SZA CLA	
01520	5335	JMP SIGPN	
01521	4262	JMS DPDSUB	
01522	7420	SNL	
01523	5775	JMP 1704	
01524	5774	JMP SROT	
01525	7300	NOISE, CLA CLL	
01526	1254	TAD ALSDN	
01527	3307	DCA LSDH	
01530	1255	TAD AMSDN	
01531	3310	DCA MSDH	
01532	1256	TAD AHSDN	
01533	3311	DCA HSDH	
01534	5774	JMP SROT	
01535	1251	SIGPN, TAD ALSDSN	
01536	3307	DCA LSDH	
01537	1252	TAD AMSDSN	
01540	3310	DCA MSDH	
01541	1253	TAD AHSDSN	
01542	3311	DCA HSDH	
01543	5774	JMP SROT	
01544	0001	SORN, 1	/SORN>0, S+N; <0, N; =0, S+N-N=S
01545	0001	SORD, 1	/SORD>0, DMA SINGLE PREC.
01546	0000	CLEAR, 0	/CLEARS MEMORY LOCATIONS STADD
01547	7200	CLA	/PLUS N. ENTERED THUSLY:
01550	1746	TAD I CLEAR	/JMS CLEAR; STADD; N
01551	3365	DCA STADD	
01552	2346	ISZ CLEAR	
01553	1746	TAD I CLEAR	
01554	7041	CIA	
01555	3366	DCA COUNTC	
01556	3765	DCA I STADD	
01557	2365	ISZ STADD	
01560	2366	ISZ COUNTC	
01561	5356	JMP -3	
01562	2346	ISZ CLEAR	
01563	7300	CLA CLL	
01564	5746	JMP I CLEAR	
01565	0000	STADD, 0	
01566	0000	COUNTC, 0	
01570	0520	/DISPLAY ROUTINE FOR TIME OF FLIGHT.	
01571	1456	/AUTOMATICALLY SCALES BOTH AXES. TAKES SUM OF N. BINS.	
01572	1454	/TAKES S+N-N, LOOKS AT ORIGINAL DATA FIELD (SING PREC)	
01573	1451	/OR AT DOUBLE PRECISION STORAGE LOCATIONS.	
01574	1647		

01575 1704  
01576 1756  
01577 0400

\*1600

01600	7300	DISPLA,	CLA CLL	
01601	3355		DCA NDIS	
01602	3362		DCA ROTF	
01603	3365		DCA NA	
01604	1354		TAD NBINA	
01605	2355		ISZ NOIS	
01606	7004		RAL	
01607	4720		SNL	
01610	5205		JMP. -3	
01611	7300		CLA CLL	
01612	3365		DCA NA	
01613	7200	STAR,	CLA	
01614	7000		NOP	
01615	7000		NOP	
01616	5222		JMP .+4	
01617	7240		CLA CMA	
01620	1362		TAD ROTF	
01621	3362		DCA ROTF	/SETS ROTF=ROTF-1 IF NO VALUE >
01622	1362		TAD ROTF	/TWO OF FULL SCALE
01623	1377		TAD (+6)	
01624	7500		SMA	
01625	5231		JMP .+4	
01626	7200		CLA	
01627	1376		TAD (-5)	/WON'T ROTATE ANY MORE THAN 5
01630	3362		DCA ROTF	
01631	7240		CLA CMA	
01632	1353		TAD START2	
01633	3356		DCA XN	/XN=START2-1
01634	4775	RET,	JMS CLEAR	
01635	1451		AL SDSN	
01636	0006		6	
01637	1364		TAD NBIND	
01640	7041		CIA	
01641	3360		DCA NBIN2	
01642	2356		ISZ XN	
01643	4774		JMS DPDADD	
01644	2360		ISZ NBIN2	
01645	5242		JMP .-3	/ADDS UP N BINS TO TRIPLE PRE
01646	5773		JMP CHECKD	
01647	1362	SROT,	TAD ROTF	
01650	7500		SMA	
01651	7041		CIA	/MAKES ROTF2=-ABS(ROTF)
01652	7450		SNA	/SKIPS ALL ROTATING IF ROTF=0
01653	5260		JMP .+5	
01654	3363		DCA ROTF2	
01655	4320		JMS TROT	
01656	2363		ISZ ROTF2	/ROTATES TRIPLE PRECISION
01657	5255		JMP .-2	/RIGHT (OR LEFT IF ROTF<0
01660	7200		CLA	
01661	1772		TAD MSDH	
01662	7440		SZA	
01663	5350		JMP BIG	
01664	1771		TAD HSDH	
01665	7440		SZA	/IF ANYTHING LEFT IN HSDH OR MSB
01666	5350		JMP BIG	/THEN DIDN'T ROTATE RIGHT ENOUGH
01667	1770		TAD LSDH	
01670	7510		SPA	
01671	7000		NOP	/IF ANY VALUE IS WITHIN 2 OF FS
01672	6063		DYL	/FLAG1 IS SET NON-ZERO

			/PREVIOUS STEP LOADS Y-AXIS
01673	7300		CLA CLL
01674	1355		TAD NDIS
01675	7041		CIA
01676	3357		DCA NN
01677	1365		TAD NA
01700	2357		ISZ NN
01701	5315		JMP ROT
01702	6053		DXL
01703	6054		DIX
01704	7300		CLA CLL
01705	1354		TAD NBINA
01706	7041		CIA
01707	1365		TAD NA
01710	2365		ISZ NA
01711	7710		SPA CLA
01712	5234		JMP RET
01713	5211		JMP 1611
01714	7000		NOP
01715	7100	ROT,	CLL
01716	7004		RAL
01717	5300		JMP SKIP
01720	0000	TROT,	O
01721	7200		CLA
01722	1362		TAD ROTF
01723	7500		SMA
01724	5326		JMP TRR
01725	5341		JMP TRL
01726	7300	TRR,	CLA CLL
01727	1771		TAD HSDH
01730	7010		RAR
01731	3771		DCA HSDH
01732	1772		TAD MSDH
01733	7010		RAR
01734	3772		DCA MSDH
01735	1770		TAD LSDH
01736	7010		RAR
01737	3770		DCA LSDH
01740	5720		JMP I TROT
01741	7300	TRL,	CLA CLL
01742	1770		TAD LSDH
01743	7004		RAL
01744	7430		SZL
01745	5350		JMP BIG
01746	3770		DCA LSDH
01747	5720		JMP I TROT
01750	2362	BIG,	ISZ ROTF
01751	7000		NOP
01752	5213		JMP STAR
01753	2001	START2,	2001
01754	0062		0062
01755	0000	NDIS,	0000
01756	0000	XN,	0000
01757	0000	NN,	0000
01760	0000	NBIN2,	0
01761	0000	FLAGD,	0
01762	0000	ROTF,	0
01763	0000	ROTF2,	0
01764	0004	NBIND,	0004

01770	1507
01771	1511
01772	1510
01773	1513
01774	1400
01775	1546
01776	7773
01777	0006

\*5000  
05000 4777 BTX, JMS TYPX  
05001 5357 CMBINT  
05002 4134 JMS INPUT  
05003 6174 6174  
05004 4407 JMS I 7  
05005 6776 FPUT FBINT  
05006 0000 FEXT  
05007 7300 CLA CLL  
05010 5022 JMP RESTOR  
05011 0000 NBTL, 0  
05012 0000 CTL, 0  
05013 7300 CLA CLL  
05014 3340 DCA NCTL  
05015 4134 JMS 134  
05016 4407 JMS I 7  
05017 6172 FPUT CTHOLD  
05020 3264 FMPPY MILL /MILL=MILLION, 10<sup>6</sup>  
05021 0000 FEXT  
05022 4407 CTLRET, JMS I 7 /TEN=10 (10)  
05023 4267 FDIV TEN  
05024 0000 FEXT  
05025 2340 ISZ NCTL  
05026 1375 TAD (-7)  
05027 1044 TAD 44  
05030 7510 SPA  
05031 5272 JMP CTLERR  
05032 1374 TAD (-4)  
05033 7540 SMA SZA / 7<=BIN EXP<=11 (10)  
05034 5222 JMP CTLRET  
05035 7450 CTLAGN, SNA  
05036 5247 JMP CTLYES  
05037 2044 ISZ 44  
05040 7300 CLA CLL  
05041 1045 TAD 45  
05042 7010 RAR  
05043 3045 DCA 45  
05044 1373 TAD (-13)  
05045 1044 TAD 44  
05046 5235 JMP CTLAGN  
05047 1372 CTLYES, TAD (-3)  
05050 1340 TAD NCTL  
05051 7510 SPA  
05052 5272 JMP CTLERR  
05053 1371 TAD (-5) / 3<=NCTL<=8?? NO: ERROR MESS  
05054 7540 SMA SZA  
05055 5272 JMP CTLERR  
05056 7200 CLA  
05057 1045 TAD 45  
05060 0370 AND (7760) /THROW AWAY 4 LSB  
05061 1340 TAD NCTL  
05062 6173 6173  
05063 5612 JMP I CTL  
05064 0024 MILL, FLTG +100.00E+04  
05065 3641  
05066 1000  
05067 0004 TEN, FLTG +100.00E-01  
05070 2400  
05071 0000  
05072 4777 CTLERR, JMS TYPX  
05073 5365 CTERR

05075	0000	CTR,	0	/COUNTING TIME READ
05076	7200		CLA	
05077	1340		TAD NCTL	
05100	7041		CIA	
05101	3341		DCA NCTL	
05102	4407		JMS I 7	
05103	5267		FGET TEN	
05104	0000		FEXT	
05105	2341	CTRRET,	1SZ NCTL	
05106	7410		SKP	
05107	5315		JMP CTROUT	
05110	4407		JMS I 7	
05111	3267		FMPY TEN	
05112	7000		FNOR	
05113	0000		FEXT	
05114	5305		JMP CTRRET	
05115	4407	CTROUT,	JMS I 7	
05116	6335		FPUT NCTL	
05117	0000		FEXT	
05120	7300		CLA CLL	
05121	6172		6170	
05122	3045		DCA 45	
05123	1367		TAD (13)	
05124	3044		DCA 44	
05125	3046		DCA 46	
05126	4407		JMS I 7	
05127	7000		FNOR	
05130	4264		FDIV MILL	
05131	3335		FMPY NCTL	
05132	7000		FNOR	
05133	0000		FEXT	
05134	5675		JMP I CTR	
05135	0000	NCTL	0	
05136	0000		0	
05137	0000		0	
05140	0000	NCTL,	0	
05141	0000	NCTL,	0	
05142	4777	CTLX,	JMS TYPX	
05143	5372		CMCT	
05144	4212		JMS CTL	
05145	5022		JMP RESTOR	
05146	4777	CTRX,	JMS TYPX	
05147	5375		CMCTR	
05150	4275		JMS CTR	
05151	1366		TAD (6)	
05152	3062		DCA 62	
05153	1365		TAD (3)	
05154	4147		JMS OUTPUT	
05155	5022		JMP RESTOR	
05156	4777	SHIFTK,	JMS TYPX	
05157	1314		CMNS	
05160	4134		JMS INPUT	
05161	3764		DCA NBIND	
05162	5144		JMP 144	

NBIND=1764  
TYPX=1200  
FBINT=346  
RESTOR=22  
CTHOLD=172

05163 1070  
05164 1764  
05165 0003  
05166 0006  
05167 0013  
05170 7760  
05171 7773  
05172 7775  
05173 7765  
05174 7774  
05175 7771  
05176 0346  
05177 1200

\*5357

05357 0211 CMBINT, TEXT "BI  
05360 1640 N  
05361 2411 TI  
05362 1505 ME  
05363 7540 =  
05364 4000 "

05365 2422 CTERR, TEXT "TR  
05366 3140 Y  
05367 0107 AG  
05370 1641 NI  
05371 3700 "

05372 0324 CMCT, TEXT "CT  
05373 7540 =  
05374 4000 "

05375 2411 CMCTR, TEXT "TI  
05376 1505 ME  
05377 7500 ="

\*1300

01300	4705	4705
01301	2000	2000
01302	3000	3000
01303	6001	ION
01304	5706	5706
01305	1546	1546
01306	1600	1600
01307	7300	CLA CLL
01310	1313	TAD KCONTI
01311	5712	JMP I 1312
01312	0432	0432
01313	7600	-200
01314	1623	CMNS,
01315	7500	="

TEXT "NS

\*1316

01316	4134	NBINX,	JMS INPUT
01317	3724		DCA I NBINAX
01320	4407		JMS I 7
01321	6576		FPUT I FNBNIX
01322	0000		FEXT
01323	5144		JMP 144
01324	1754	NBINAX,	1754

01325	4134	PARALD,	JMS INPUT
01326	4407		JMS I 7
01327	6736		FPUT I FDISTX
01330	0000		FEXT
01331	4134		JMS INPUT
01332	4407		JMS I 7
01333	6737		FPUT I FDTX
01334	0000		FEXT
01335	5740		JMP I TOT
01336	0354	FDISTX,	354
01337	0351	FDTX,	351
01340	0203	TOT,	203
01341	7201	SPN,	CLA IAC
01342	3752		DCA I SORNX
01343	5144		JMP 144
01344	7 240	NOISE,	CLA CMA
01345	3752		DCA I SORNX
01346	5144		JMP 144
01347	7300	SIGNAL,	CLA CLL
01350	3752		DCA I SORNX
01351	5144		JMP 144
01352	1544	SORNX,	1544
01353	7201	SP,	CLA IAC
01354	3765		DCA I SORDX
01355	1367		TAD T000
01356	3766		DCA I STARTX
01357	5144		JMP 144
01360	7240	DP,	CLA CMA
01361	3765		DCA I SORDX
01362	1370		TAD T00T
01363	3766		DCA I STARTX
01364	5144		JMP 144
01365	1545	SORDX,	1545
01366	17 53	STARTX,	1753
01367	2001	T000,	2001
01370	3002	T00T,	3002

\*5200

05200	0401	CMFULL, TEXT /DA
05201	2401	TA
05202	4010	H
05203	0123	AS
05204	4022	R
05205	0501	EA
05206	0310	CH
05207	0504	ED
05210	4006	F
05211	2514	UL
05212	1440	L
05213	0417	DO
05214	2502	UB
05215	1405	LE
05216	4020	P
05217	2205	RE
05220	0311	CI
05221	2311	SI
05222	1716	ON
05223	7340	;
05224	0417	DO
05225	1624	NT
05226	4003	C
05227	1716	ON
05230	2411	TI
05231	1625	NU
05232	0500	E/
05233	1726	CMOVER, TEXT /OV
05234	0522	ER
05235	0614	FL
05236	1727	OW
05237	3700	←
05240	4340	#
05241	0331	CY
05242	0315	CL
05243	0523	ES
05244	7500	=

RSW=6171

LCW=6170